Half Metals

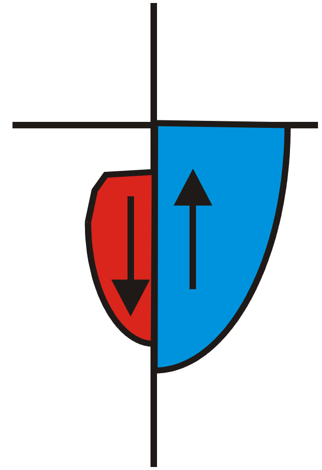

- One spin band present at E_f
- MTJs with ½-metals show large effects
  - 200% MR with 1 electrode
  - M-I transition with both electrodes
- Useful ½ metals
  - High Curie temperature
  - Well behaved magnetism
  - Interface stability
  - Thermal stability
  - Defect tolerant

Feng J. Appl. Phys. 91 8340 (2002)

- d-d gap
  - Fe_3O_4
  - $MnFe_2O_4$
    - Singh PRB **65** 064432 (2002)
  - $Fe_xCo_{(1-x)}S_2$
    - Mazin APL **77** 3000 (2000)
- Charge transfer gap
  - CrO_2
  - Manganites
- Covalent gap
  - Semi-Heusler Family
    - NiMnSb
    - PtMnSb

Stuart Parkin
July 7, 2003

Crystal and Band Structure of Fe_3O_4

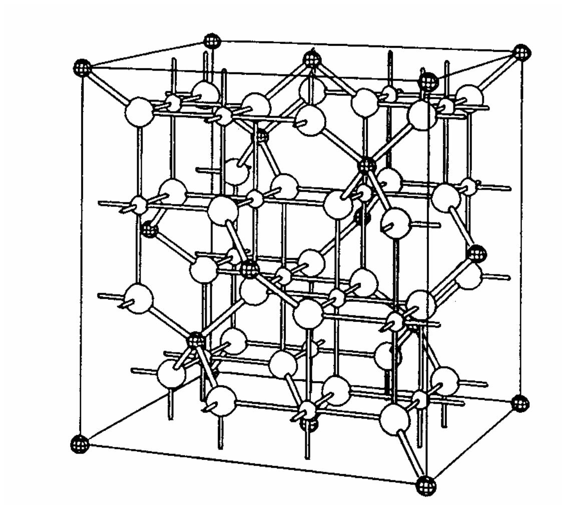

A site cation
B site cation
Anion

Yanase & Siratori, 1984

Inverse Spinel: fcc close packed O
A site: Tetrahedral Fe^{3+}
B site: Octahedral Fe^{3+} and Fe^{2+}

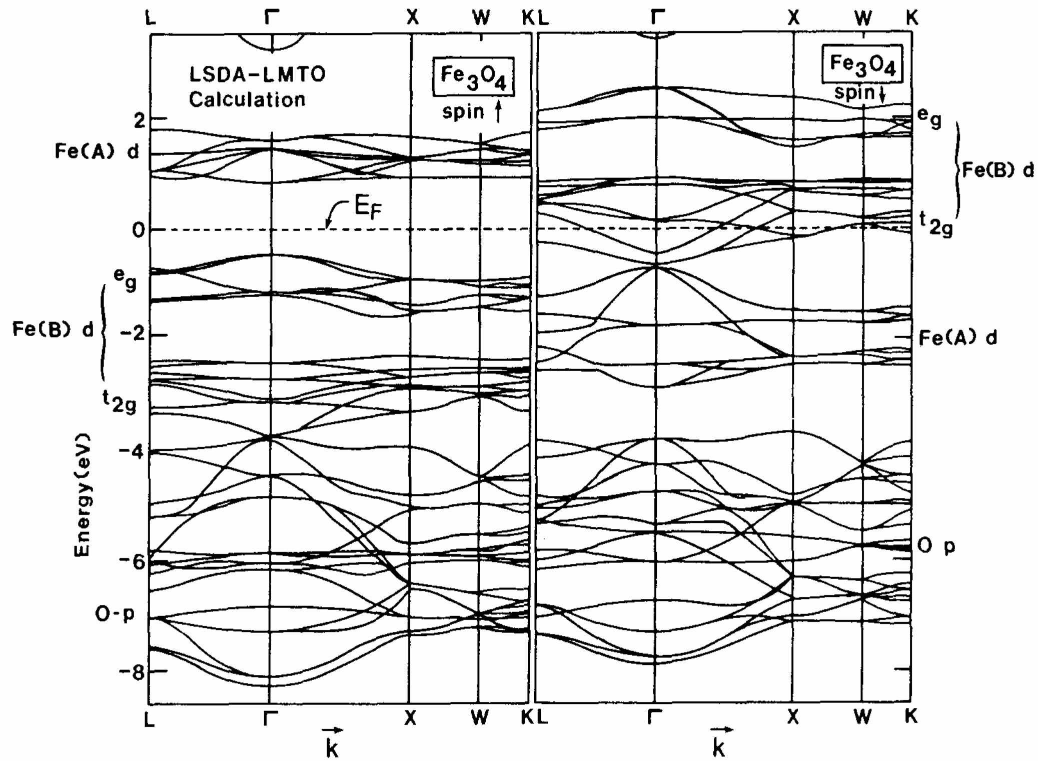

- Spin polarized electron bands from local spin density LMTO calculation [Zhang & Satpathy, 1991]
- Half metallic nature of Fe_3O_4 confirmed by recent fully relativistic first principles band structure calculations [Art Freeman]
- Only minority-spin electrons are present at the Fermi Energy

Magnetic Tunnel Junction with 24 Å MgO barrier: Normal and Inverse MR

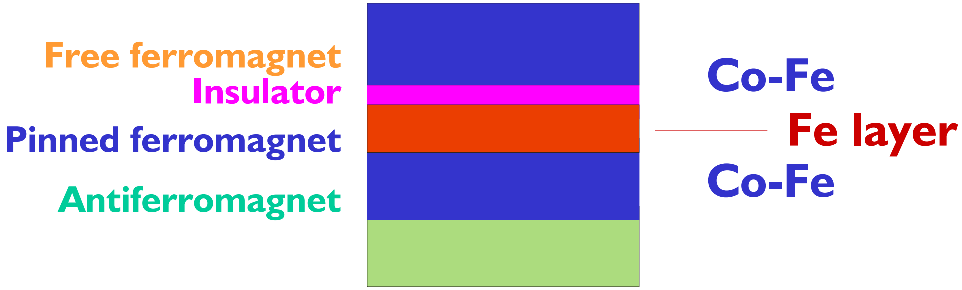

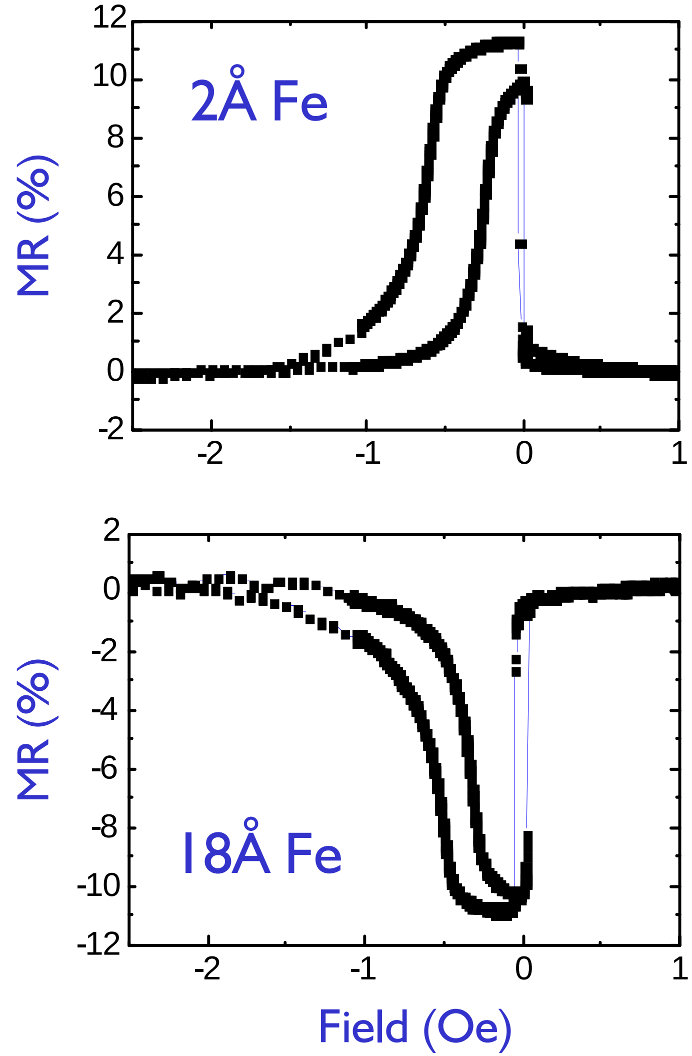

- negative spin polarization of -48%

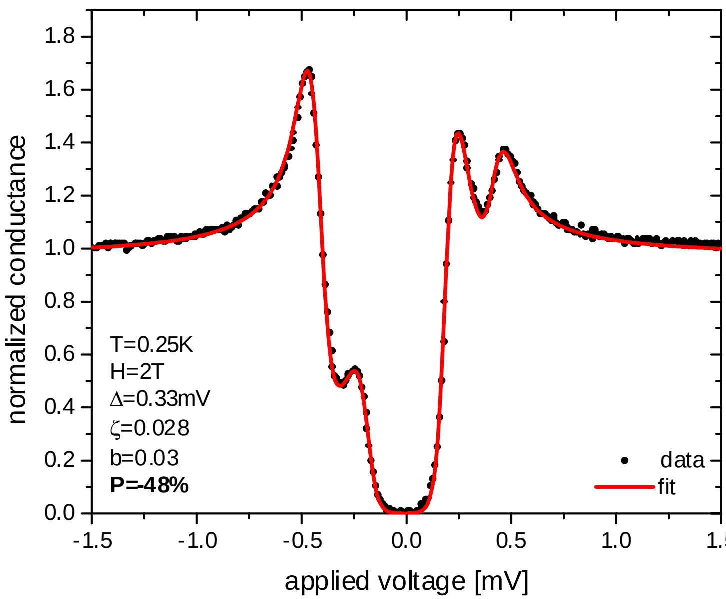

- Increased polarization for thicker layers of Fe_3O_4
- Magnetite layer is magnetically saturated as measurement is taken in an external field of 2T

Stuart Parkin
July 7, 2003

MTJ with Fe_3O_4 Electrode

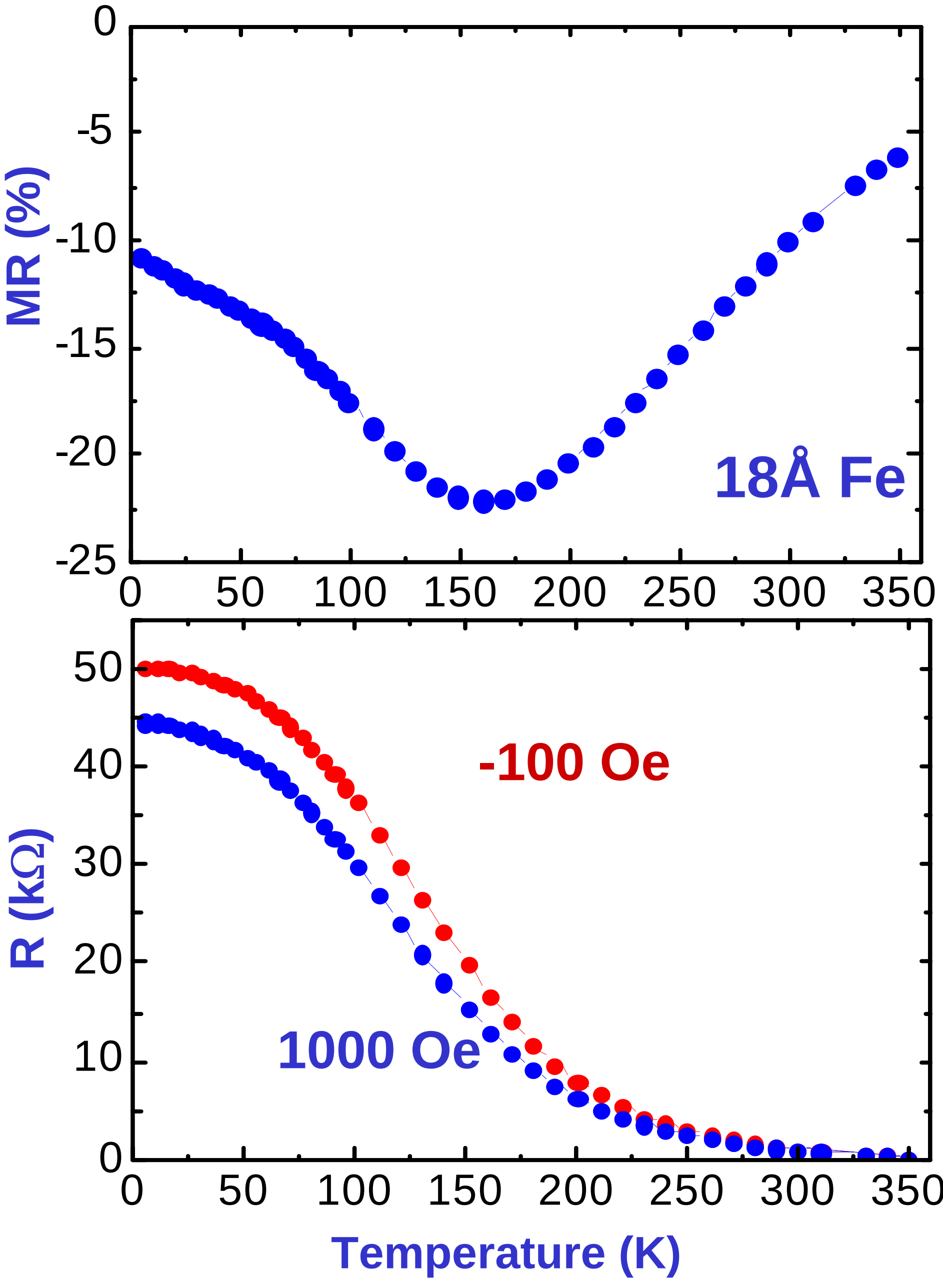

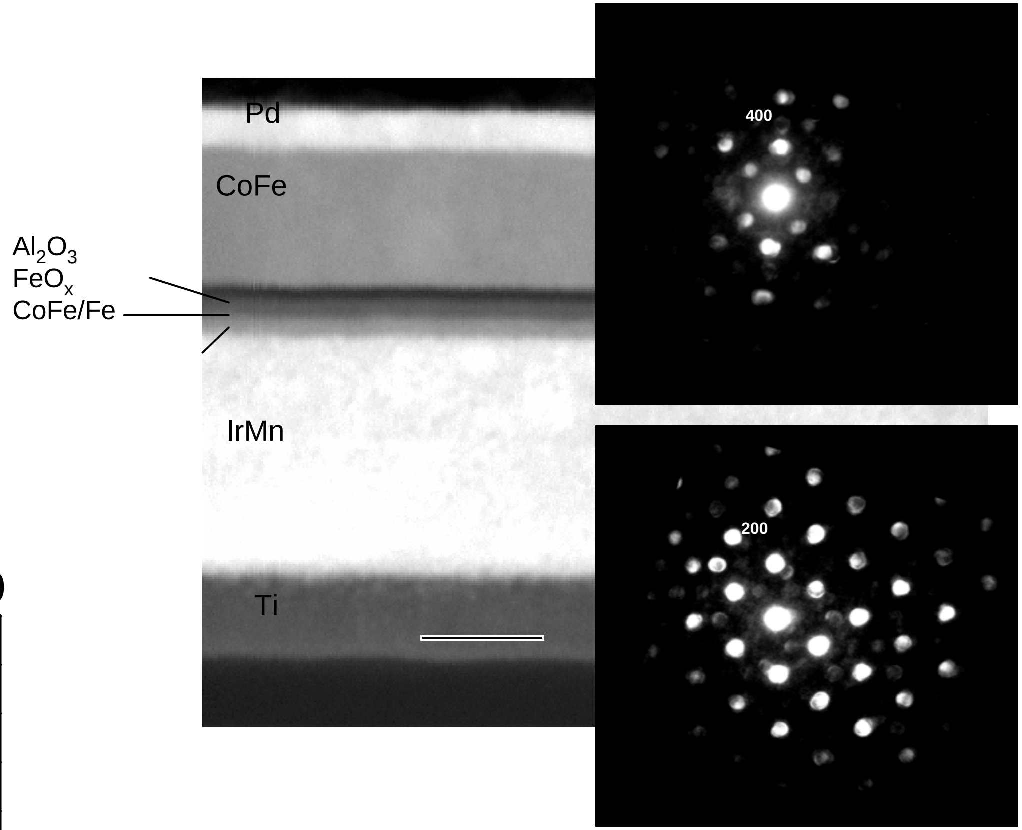

Energy filtered XTEM
→Thin [001] oriented Fe_3O_4 layer formed at interface between Fe and oxide barrier
→No TMR for [111] oriented Fe_3O_4

Amorphous ferromagnetic electrodes

- Why amorphous?
  - Low coercivity
  - Low magnetization
  - Uniform
  - Low magnetostriction
  - High thermal stability
- Loss of some spin polarization due to metalloid atoms
- Thin interface layer improves performance

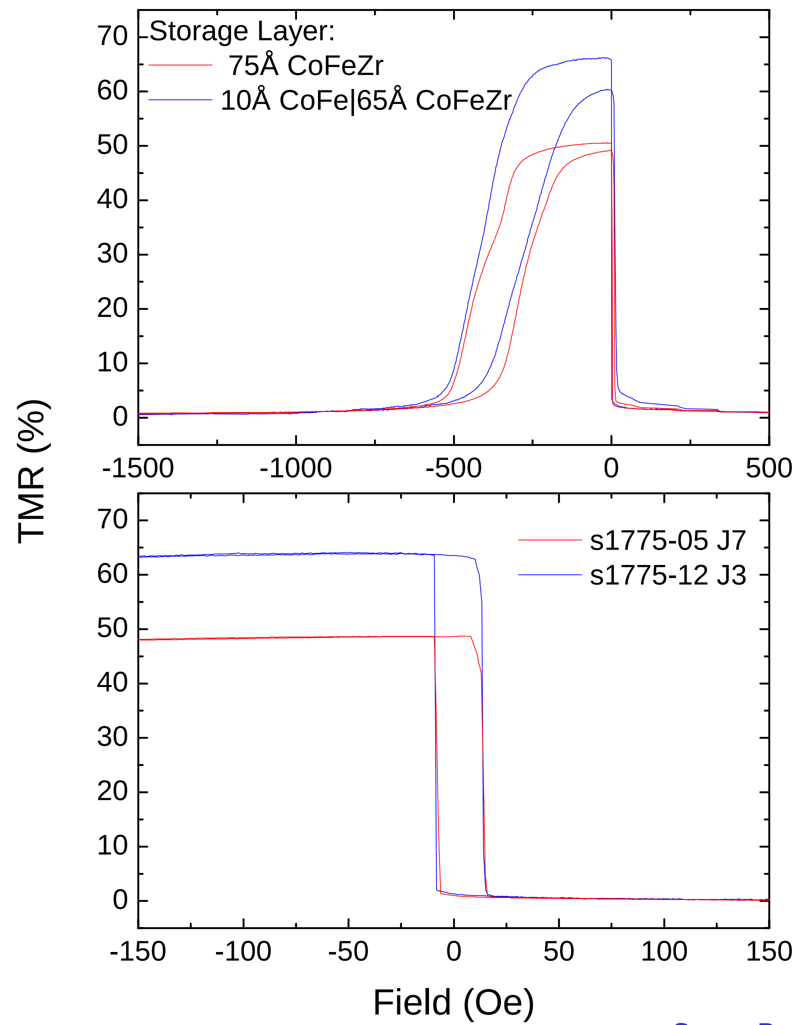

Stuart Parkin
July 7, 2003

Thin amorphous layers

- Thin CoFe layers are amorphous between Al_2O_3 and CoFeB for t < 20 Å

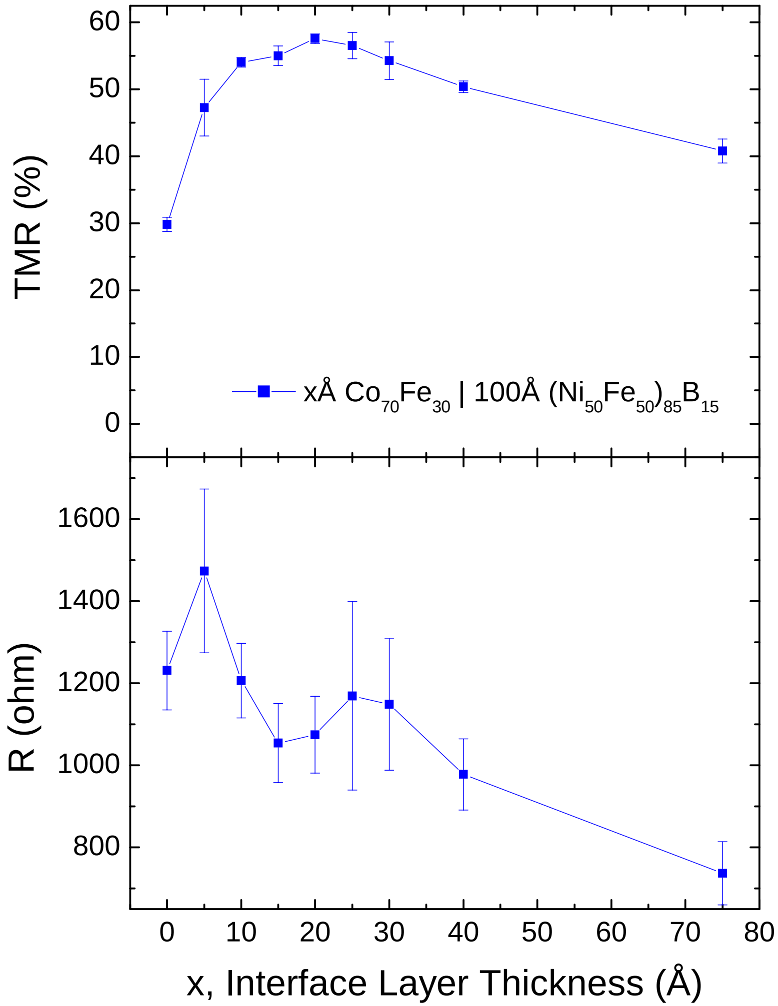

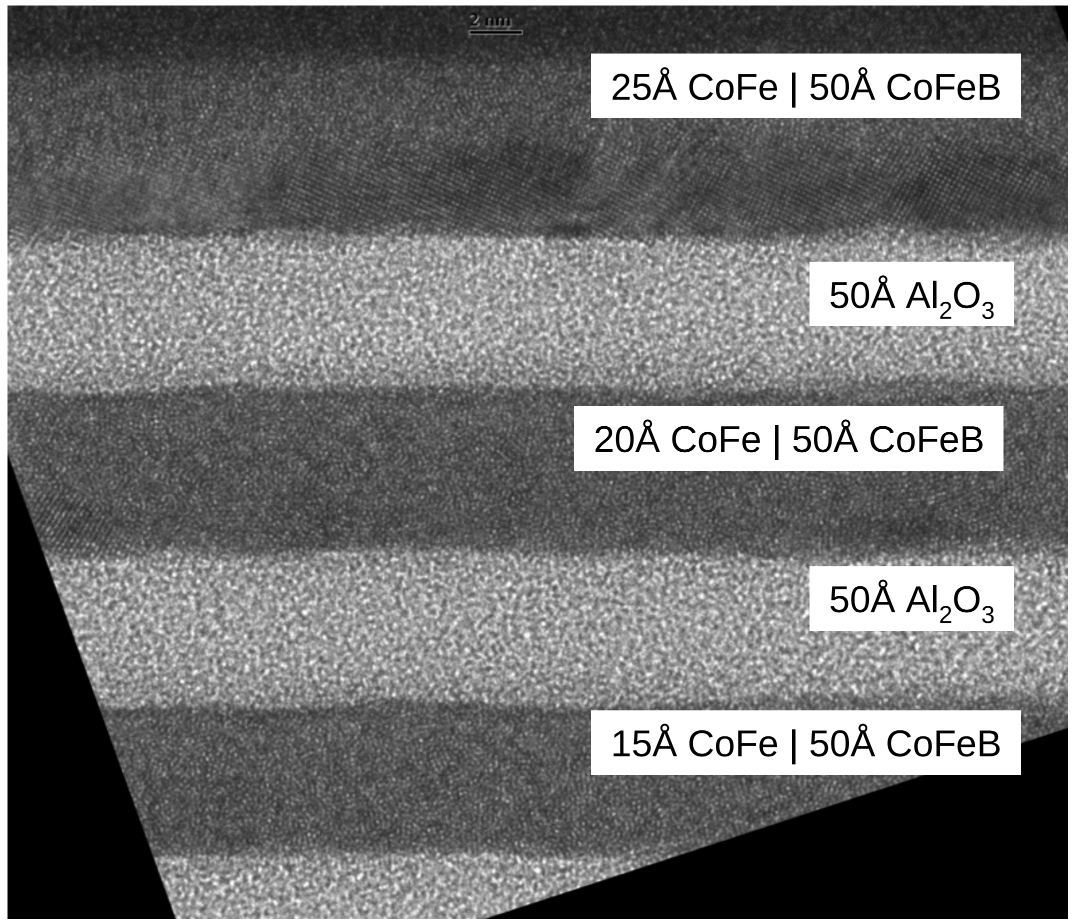

XTEM: Phil Rice

Stuart Parkin
July 7, 2003

Soft X-ray Emission Spectroscopy (SXES)

conventional
x-ray fluorescence
→ partial local DOS

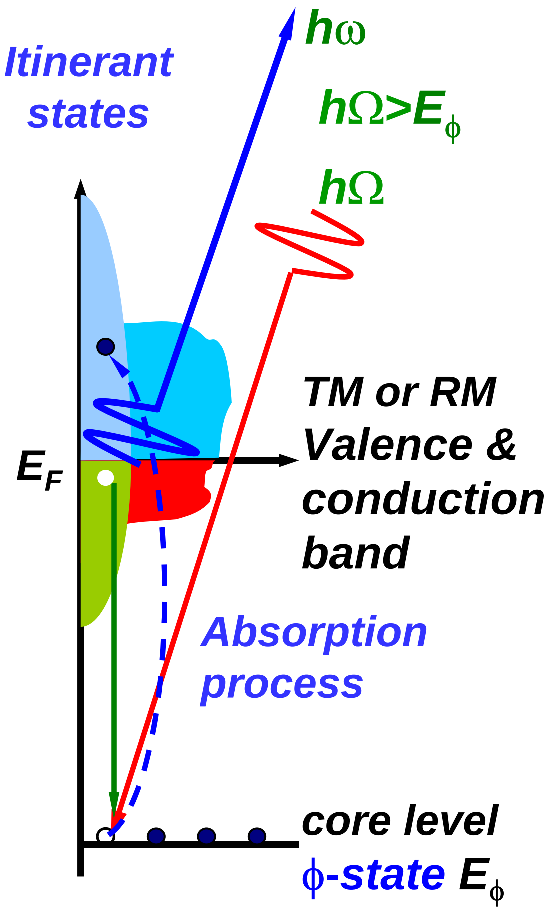

resonant x-ray emission
elastic scattering
(recombination)

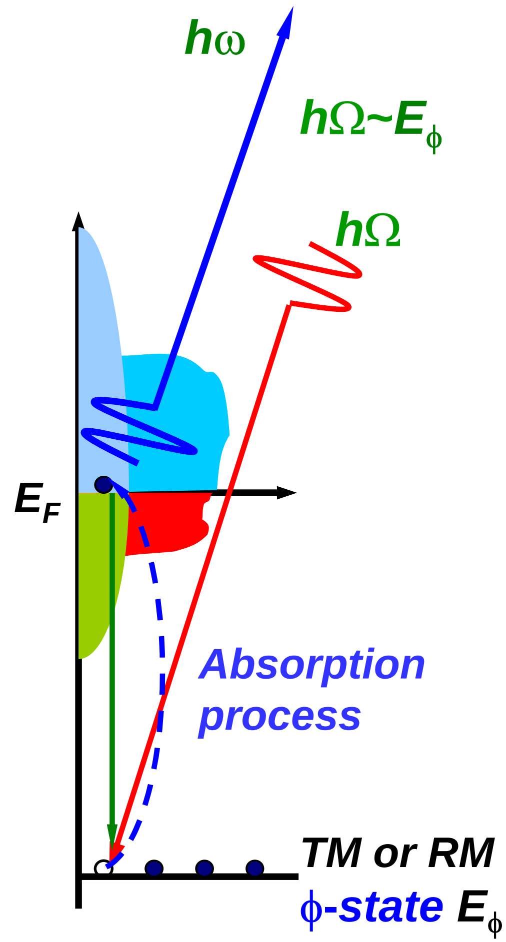

Stuart Parkin
July 7, 2003

Resonant X-ray Emission Near Fe 2p edge

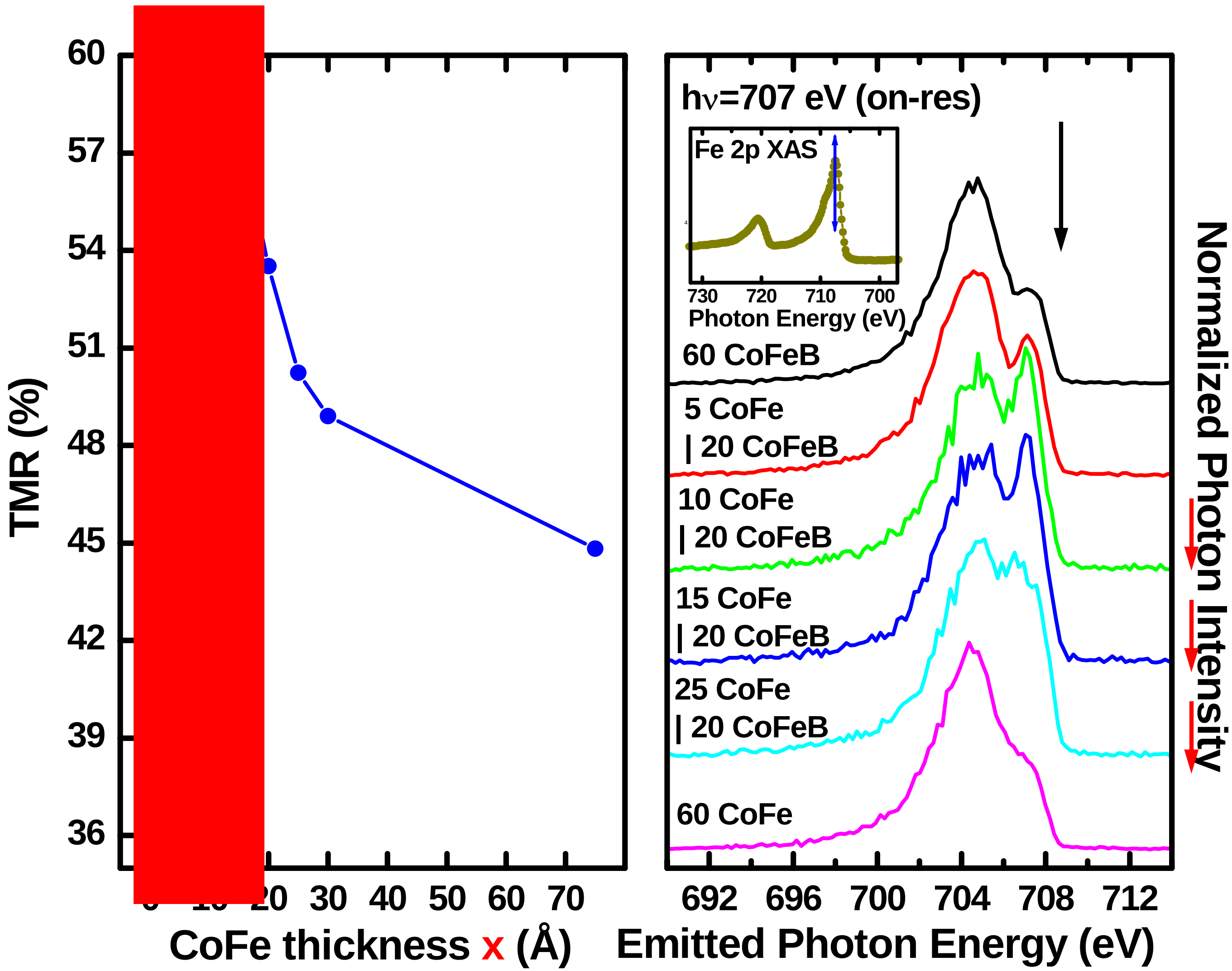

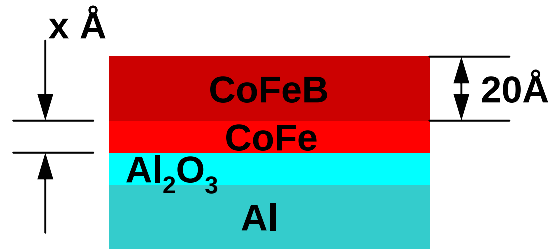

- ***Enhancement of spectral feature at Fermi level for on-resonant XES (Fe 3d partial DOS) at x= 15~20 Å → same range of thickness for enhanced TMR***

- ***V. L. Moruzzi et al. (1983) find enhanced dos for disordered CoFe***

Resonant X-ray Emission Near Fe 2p Edge

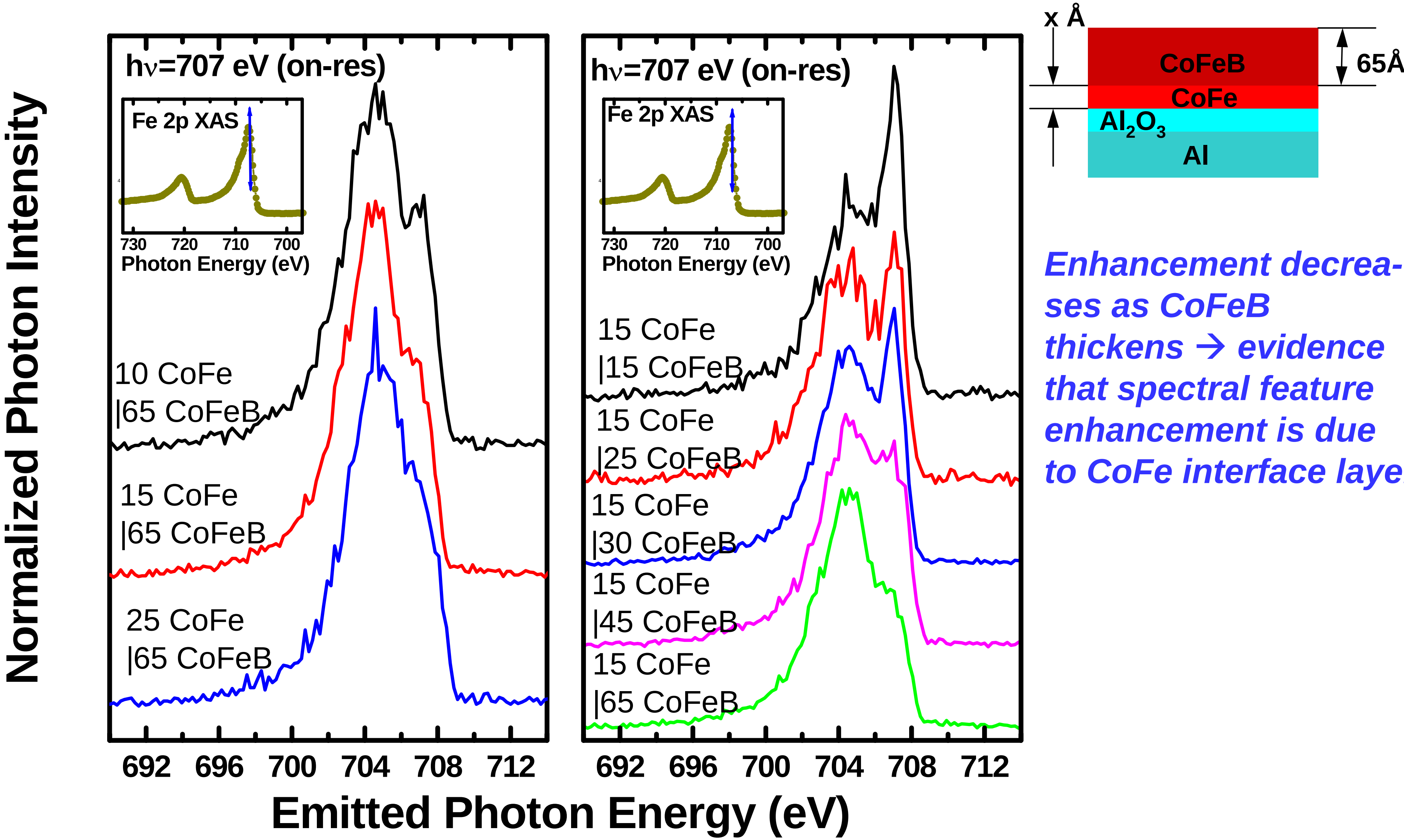

Enhancement decreases as CoFeB thickens → evidence that spectral feature enhancement is due to CoFe interface layer

Stuart Parkin
July 7, 2003

Resonant x-ray emission near Co 2p edge

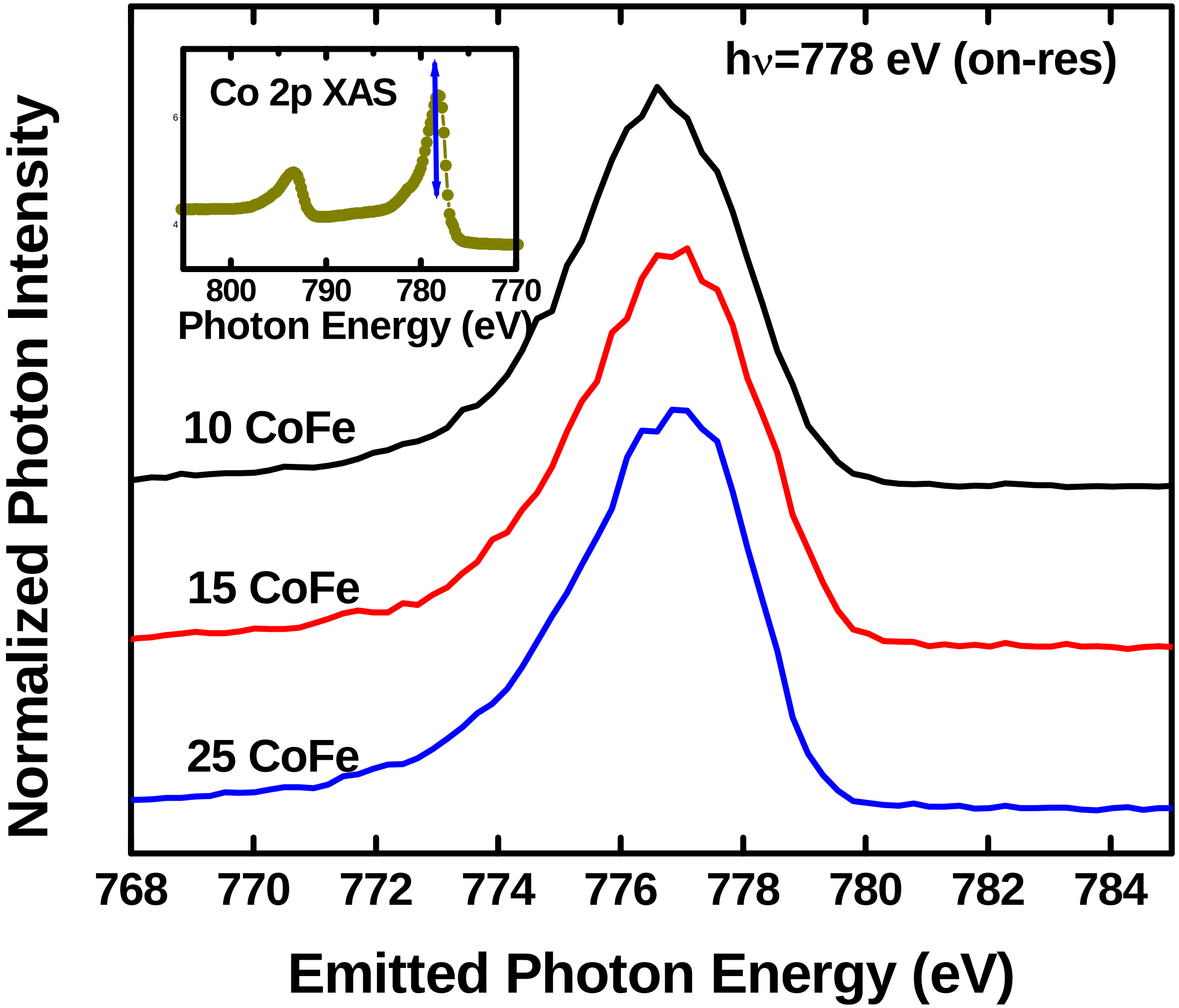

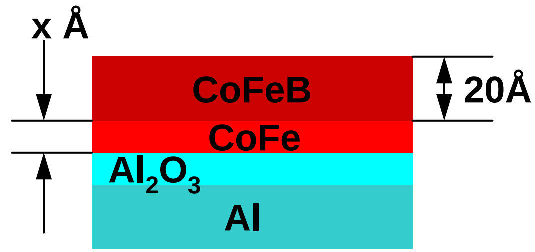

- *no change of Fermi level feature → evidence that Co LDOS does not change at Fermi level with amorphization; consistent with unchanged Co local magnetic moment in CoFe alloys*

[C. Paduani et al, J.A.P. 86, 578 (1999); J. M. MacLaren et al, JAP 85, 4833 (1999)]

Why are Magnetic Tunnel Junctions Interesting?

Perpendicular current flow
→ ideal for ultra high density recording (narrow read gap)

Much wider range of materials possible (c.f. GMR)

Interfacial phenomenon: very thin stacks (c.f. GMR)

Weak temperature dependence

No theoretical limit to Tunneling Magnetoresistance!

- GMR: 1990: 10%; Today: 15-20% (simple spin valve)
- TMR: 1975: 2% (4K); 1995: 10% ; 1997: 48%;
  Today: >220% at 300K

→Magnetic Tunnel junctions: game-changer!

Previous MRAM Approaches: Ferrite Core and AMR RAM

Core Memory (1950s)

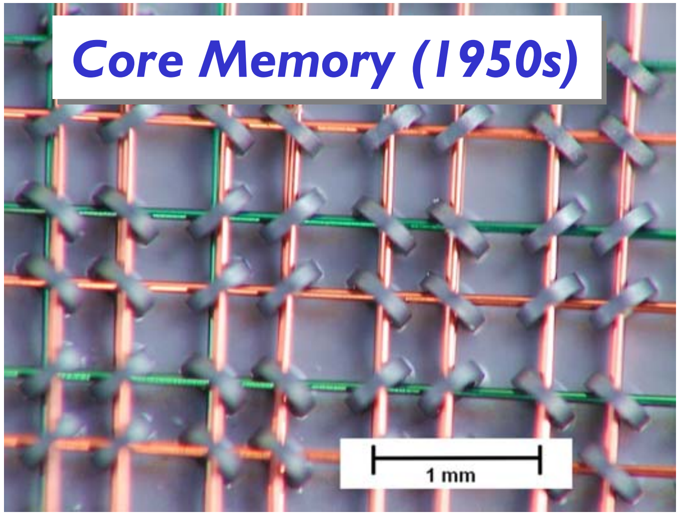

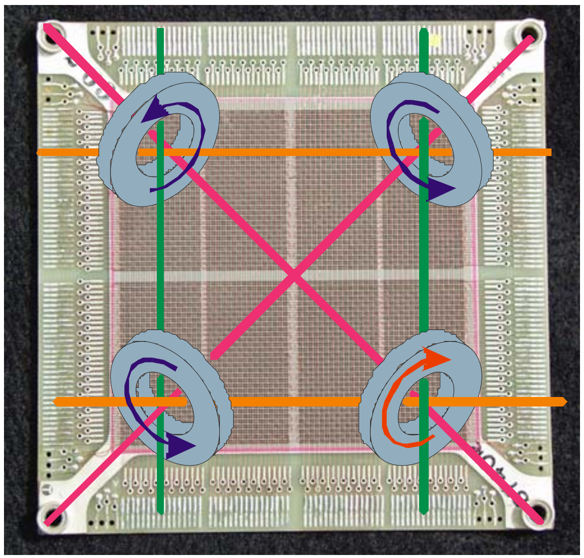

2-D array of ferrite cores with write and sense wires

Anisotropic MR (AMR) Memory (1980s)

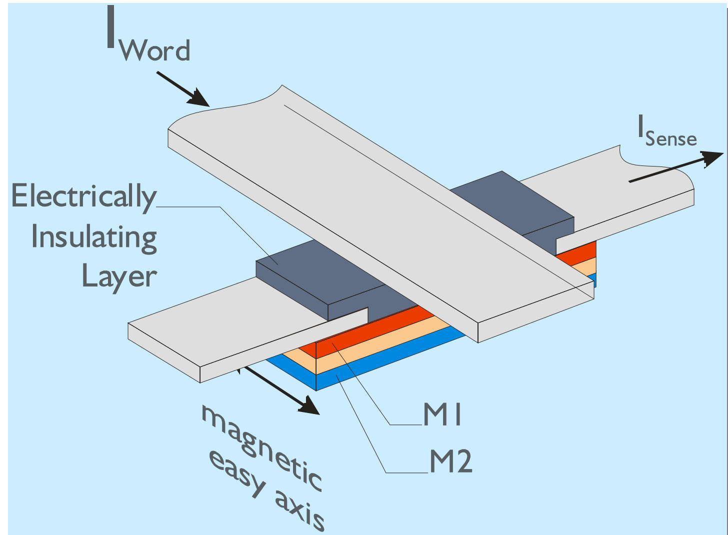

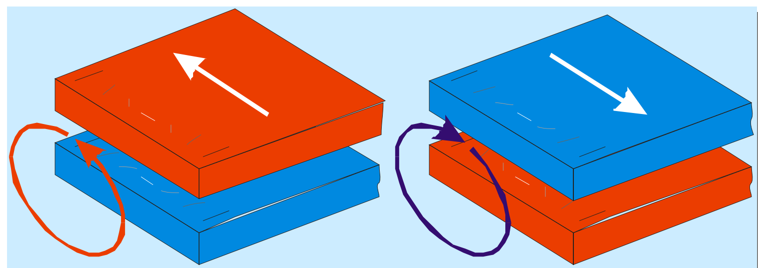

Flux closed pair of magnetic thin films

Stuart Parkin

Cross-point Architecture: Coincident Field Selection for Writing MTJ Cell

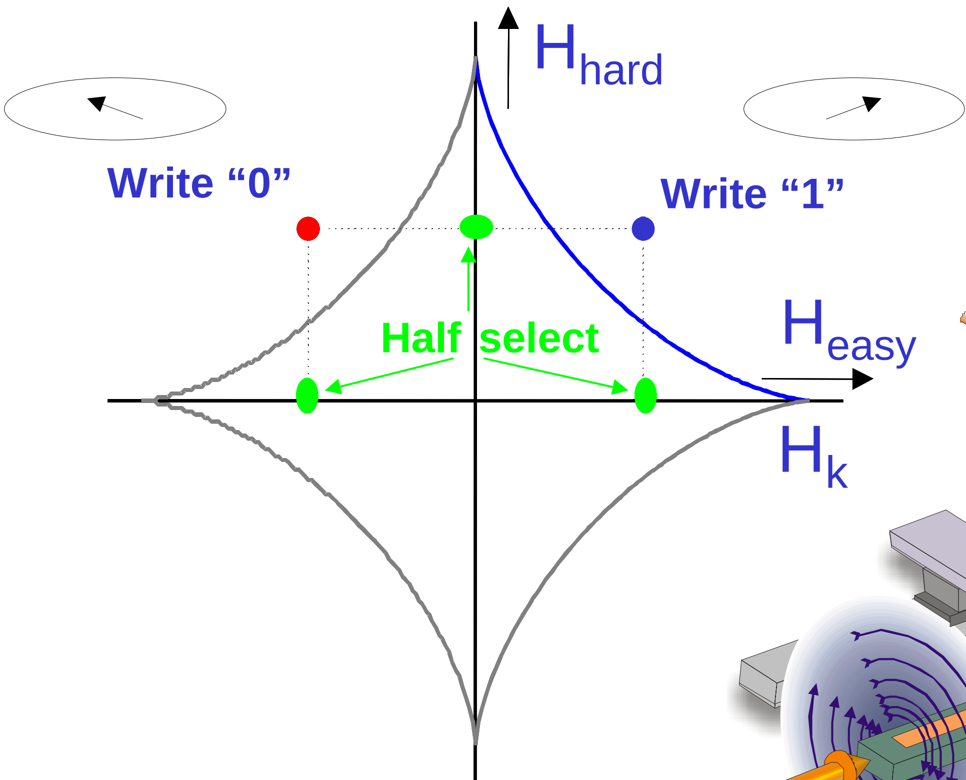

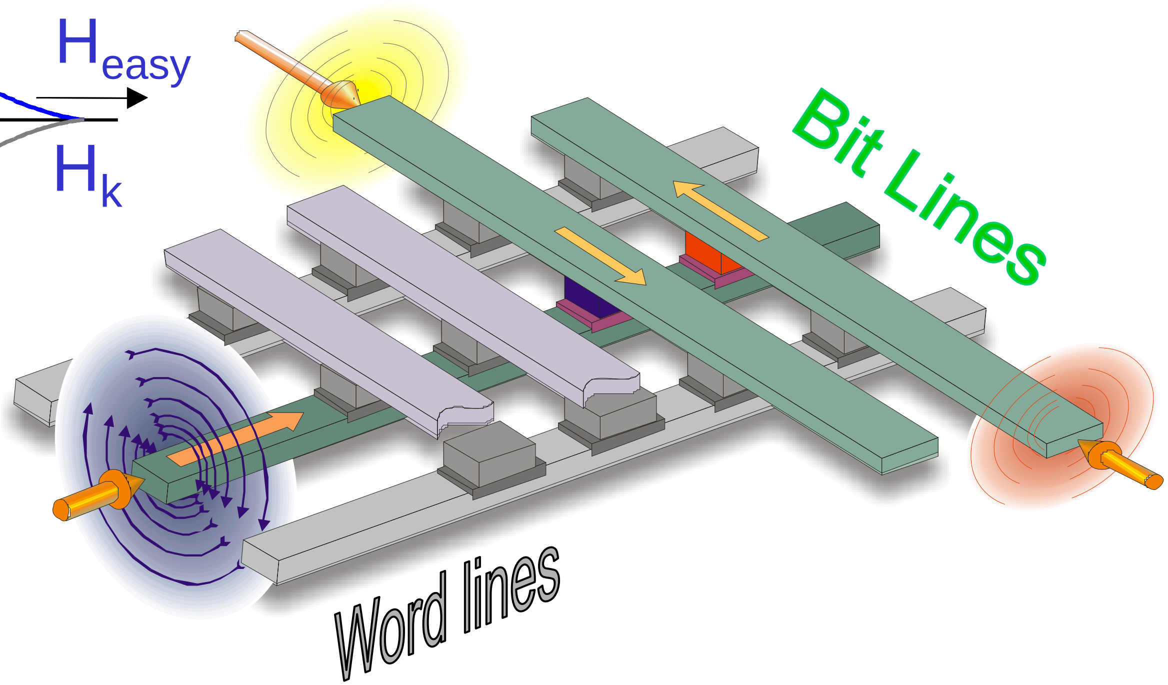

Stuart Parkin
July 7, 2003

Flux Closure Issues and Remedies in MTJs

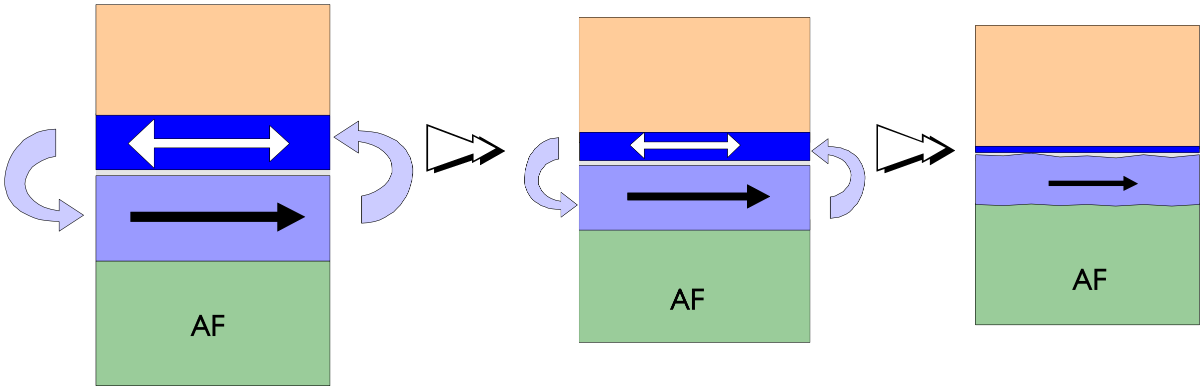

Reduce magnetostatic interaction → reduce FM layer thicknesses

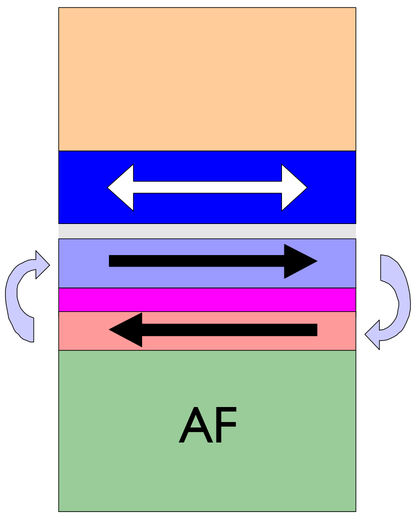

Use AP (Anti-parallel) pinned FM layer e.g. FM/Ru or FM/Os

Ref: Parkin & Heim, US patent #5,465,185 (filed 1991)
Parkin US patent (filed 1998)

Indirect Exchange Coupling via non-magnetic metals

RKKY coupling: magnetic impurity in nonmagnetic metal

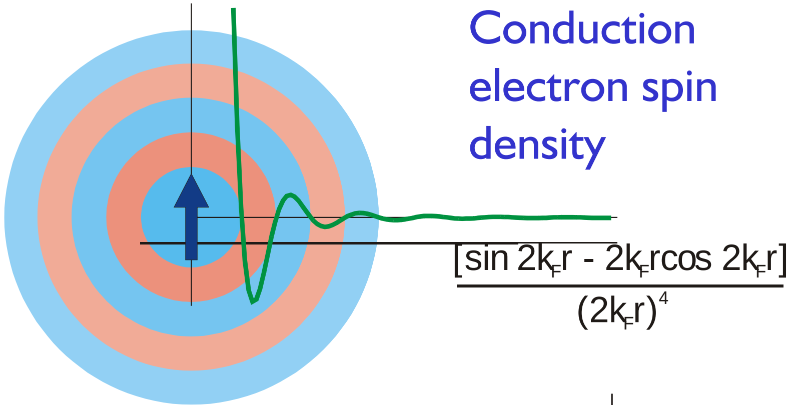

Conduction electron spin density

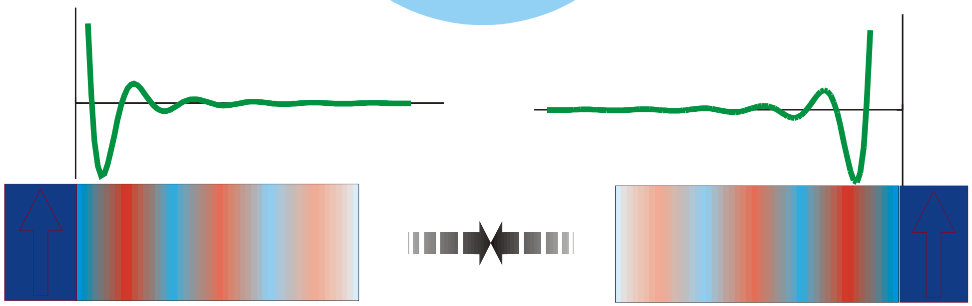

Spin density wave from scattering at interface between magnetic and non-magnetic layers

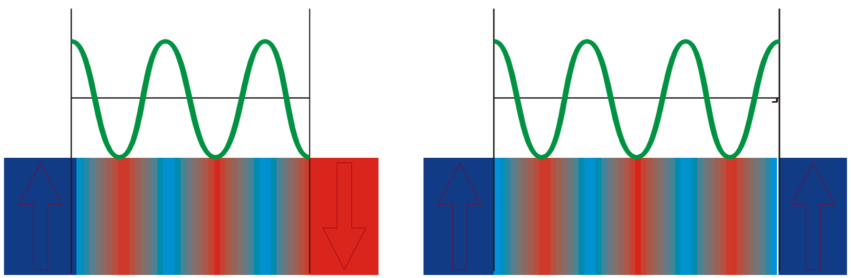

Coupling of magnetic layers via non-magnetic spacer:sign, magnitude depend on spacer thickness

Stuart Parkin
July 7, 2003

First Observation of Oscillatory Coupling and GMR in Metallic Multilayers

Parkin et al, Phys. Rev. Lett. 64, 2304 (1990)

Oscillatory coupling - Ru

Oscillatory coupling - Cr

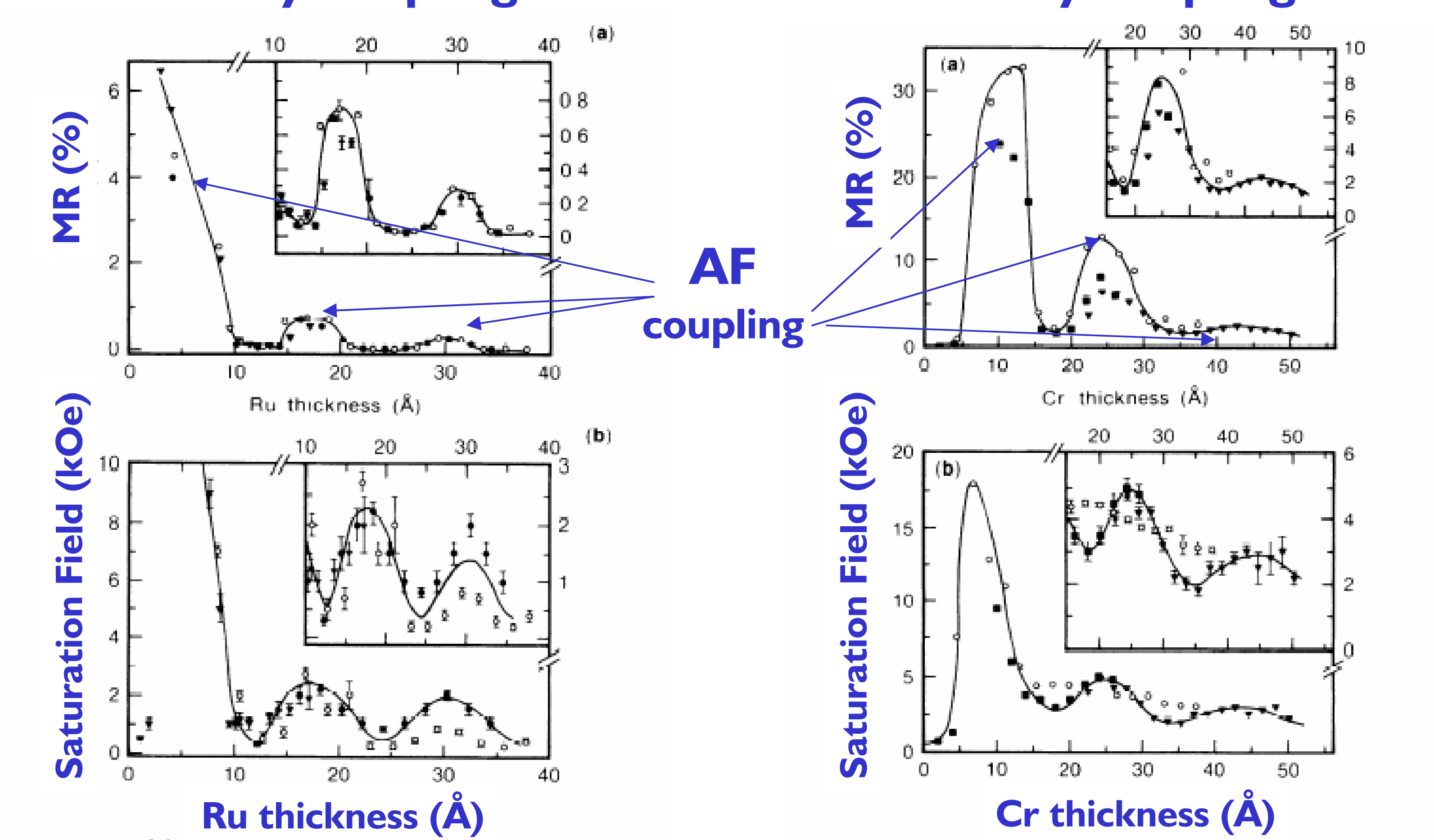

FIG. 3. (a) Transverse saturation magnetoresistance (4.5 K) and (b) saturation field (300 K) vs Ru layer thickness for structures of the form Si(111)/(100 Å) Ru/[20 Å) Co/t_{Ru} Ru]$_{20}$/(50 Å)Ru deposited at temperatures of ●, 40 °C; ○, 125 °C; ×, 200 °C.

FIG. 4. (a) Transverse saturation magnetoresistance (4.5 K) and (b) saturation field (4.5 K) vs Cr layer thickness for three series of structures of the form Si(111)/(100 Å) Cr/[(20 Å) Fe/t_{Cr} Cr]$_N$/(50 Å) Cr, deposited at temperatures of △,■, 40 °C (N=30); ○,125 °C (N=20).

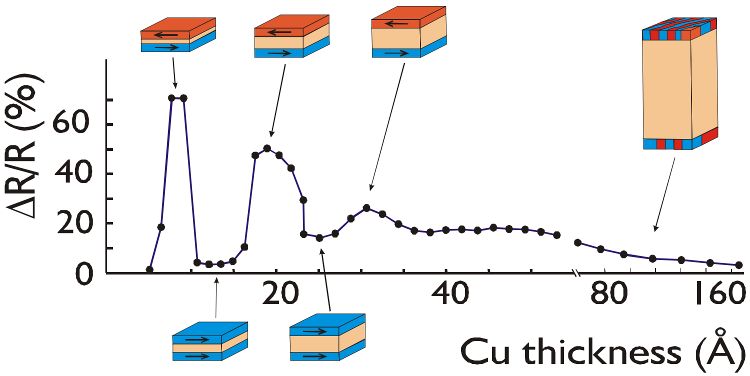

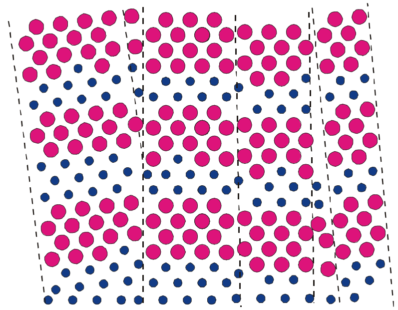

Polycrystalline

S.S.P. Parkin et al,
Phys. Rev. Lett. 66, 2152 (1991)

Oscillations in GMR: Polycrystalline vs. Single Crystal Co/Cu Multilayers

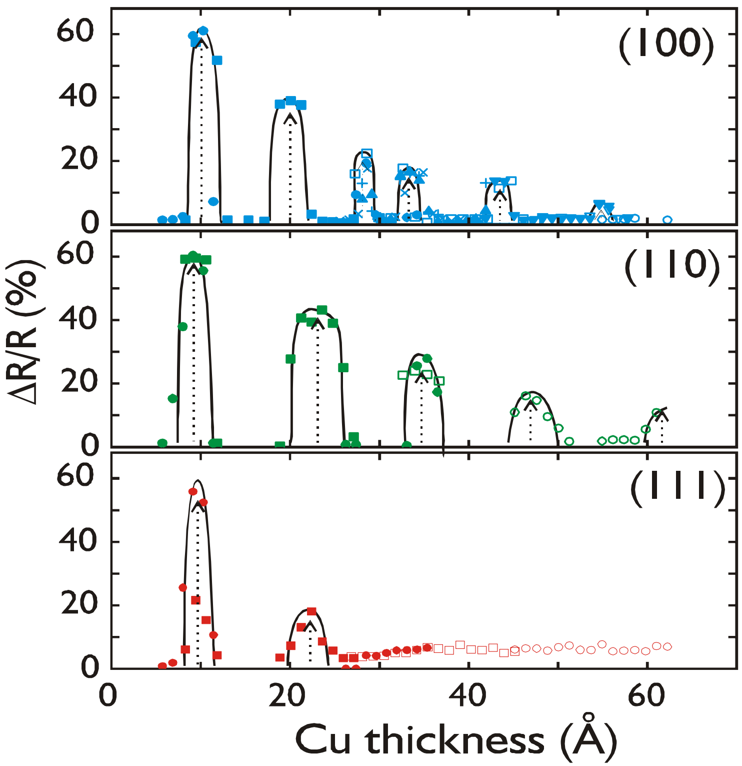

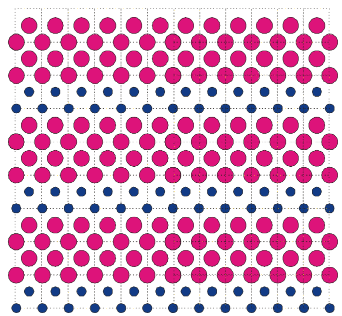

Single crystalline

S.S.P. Parkin

Sputter deposited on MgO(100), MgO(110) and Al_2O_3 (0001) substrates using Fe/Pt seed layers deposited at 500C and Co/Cu at ~40C

Stuart Parkin
July 7, 2003

Oscillatory Exchange Coupling Strength: Variation across Periodic Table

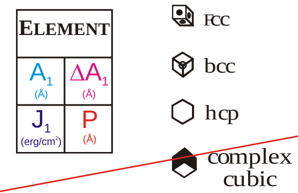

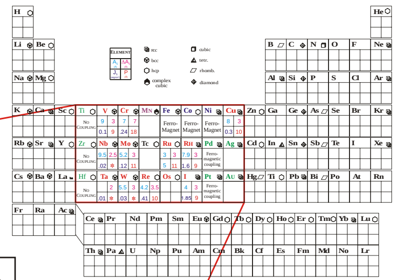

Element	Structure	A_1 (Å)	ΔA_1 (Å)	J_1 (erg/cm²)	P (Å)
Ti	hcp	No coupling			
V	bcc	9	3	0.1	9
Cr	bcc	7	7	.24	18
Mn	complex cubic				
Fe	bcc	Ferro-magnet			
Co	hcp	Ferro-magnet			
Ni	fcc	Ferro-magnet			
Cu	fcc	8	3	0.3	10
Zr	hcp	No coupling			
Nb	bcc	9.5	2.5	.02	*
Mo	bcc	5.2	3	.12	11
Tc	hcp				
Ru	hcp	3	3	5	11
Rh	fcc	7.9	3	1.6	9
Pd	fcc	Ferro-magnetic coupling			
Ag	fcc				
Hf	hcp	No coupling			
Ta	bcc		2	.01	*
W	bcc	5.5	3	.03	*
Re	hcp	4.2	3.5	.41	10
Os	hcp				
Ir	fcc	4	3	1.85	9
Pt	fcc	Ferro-magnetic coupling			
Au	fcc				

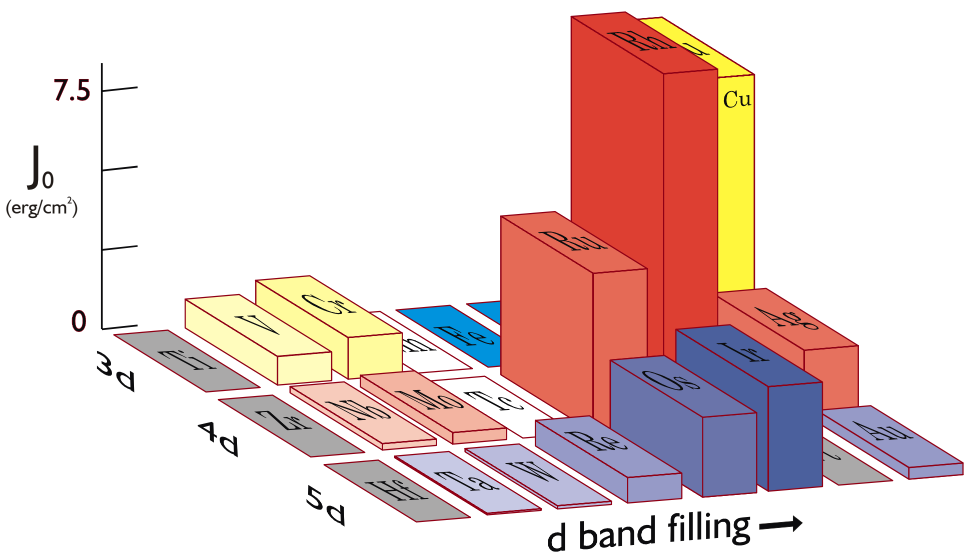

Ref: S.S.P. Parkin,
Phys. Rev. Lett. 67, 3598 (1991)

Stuart Parkin
July 7, 2003

Néel Orange-peel Coupling

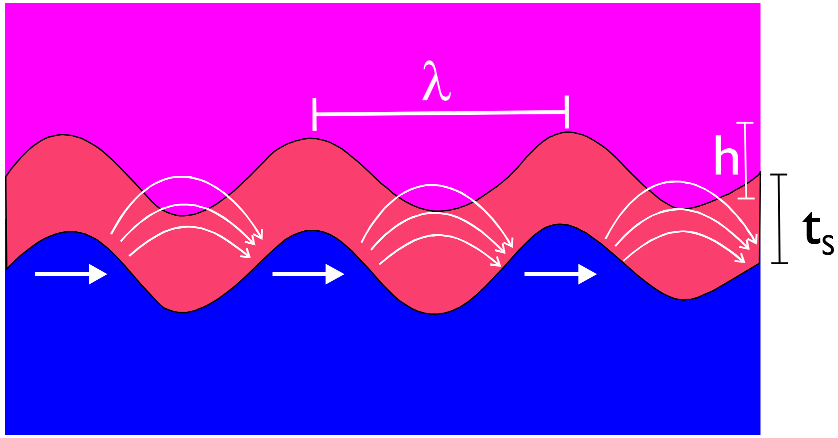

Correlated roughness leads to ferromagnetic coupling

Néel coupling field → $$H_N = \frac{\pi^2}{\sqrt{2}}\left(\frac{h^2}{\lambda t_F}\right) M_S \exp(-2\pi\sqrt{2}t_s/\lambda)$$

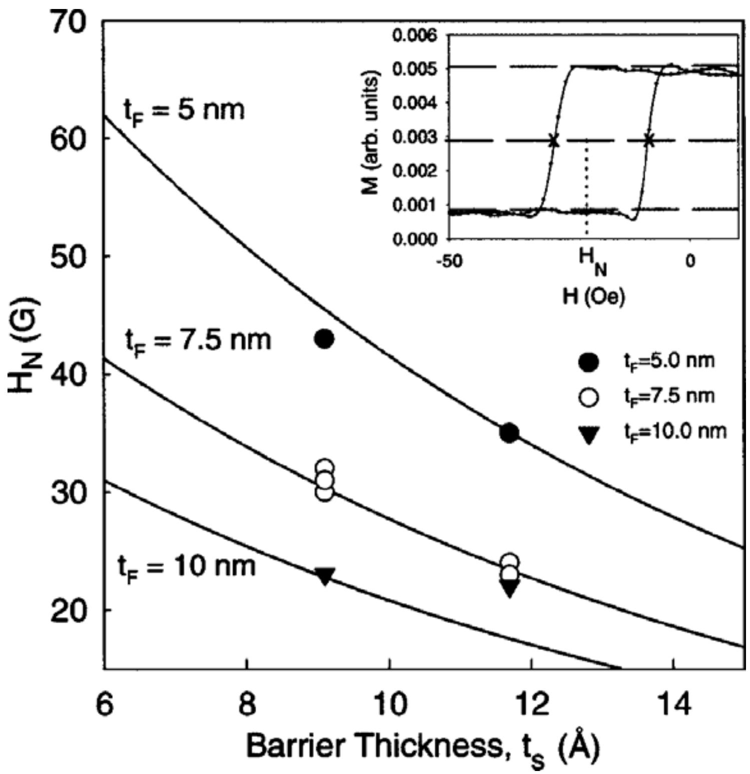

Coupling field, H_N, decreases with increasing thickness of ferromagnetic layer and tunnnel barrier

Schrag et al Appl. Phys. Lett. (2000)

Balancing Néel and Magnetostatic Fields in MTJs using Oscillatory Interlayer Coupling

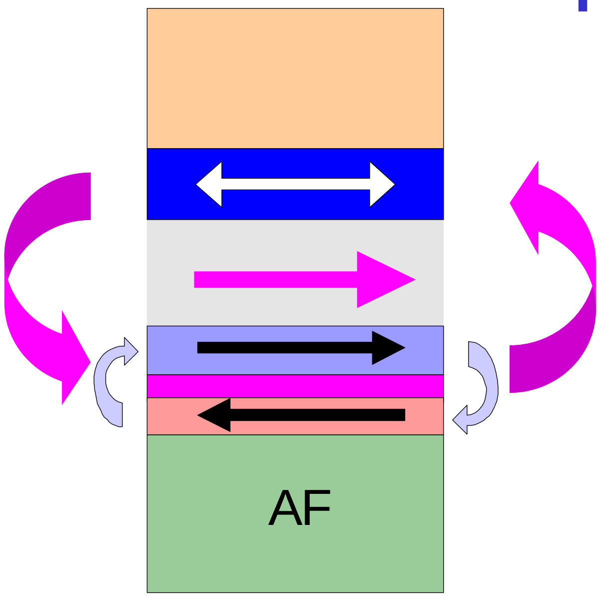

The magnetic hysteresis loop offset field is tuned to zero by balancing the dipolar and Neel coupling fields

Chiplet CA, 0.375 x 0.75 (μm)^2

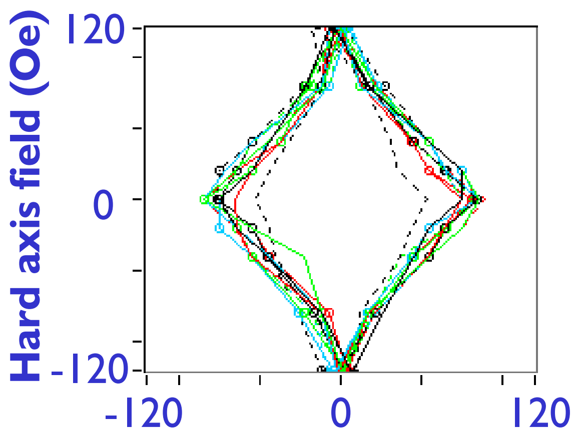

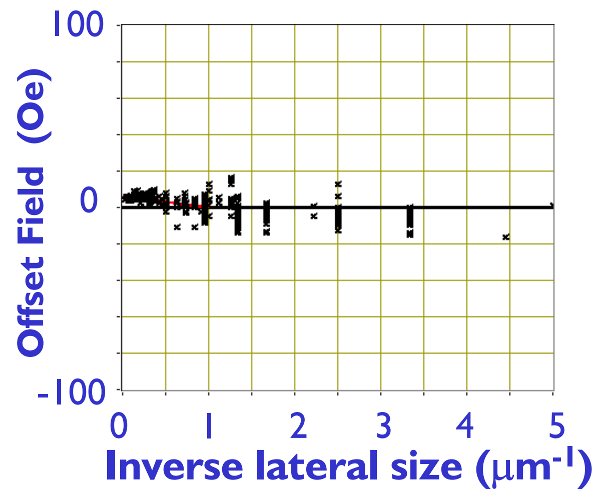

- **MTJs with Improved Magnetic Switching Characteristics**
  - **using anti-parallel pinned (AP) ferromagnetic layer**
  - **Patterned AP pinned MTJ structures display highly symmetric astroid with no offset field**

Stuart Parkin
July 7, 2003

Giant Magnetoresistance Head

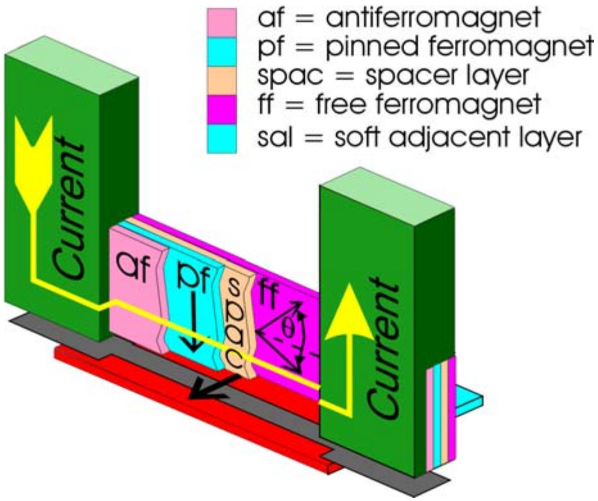

Current spin valve GMR head uses
- PtMn exchange bias layer
- CoFe/Ru/CoFe pinned layer
- Cu spacer layer
- CoFe/NiFe free layer
- Various underlayers and overlayers

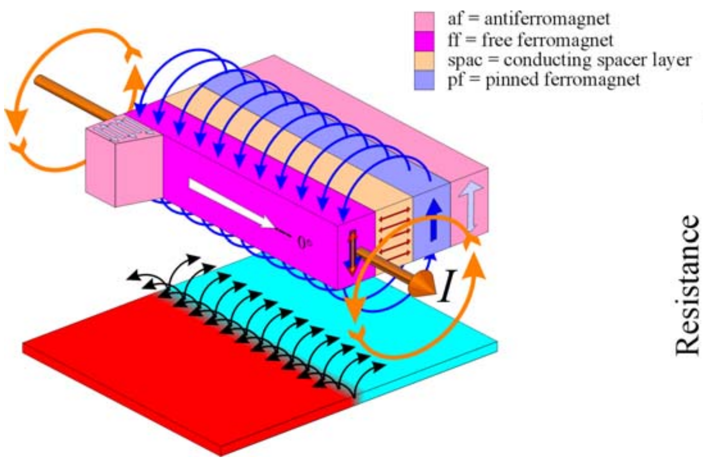

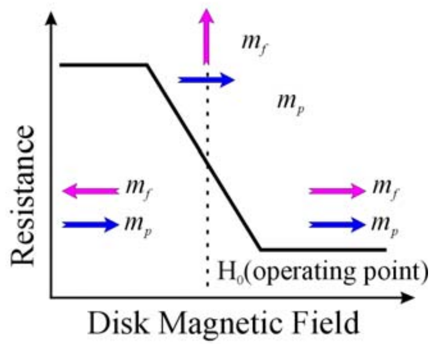

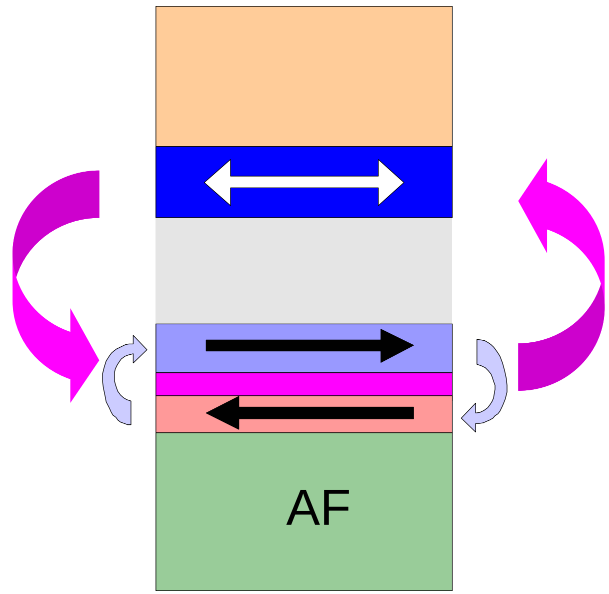

Magnetization Creep in Exchange Biased and Hard/Soft MTJ

Exchange Bias Layer

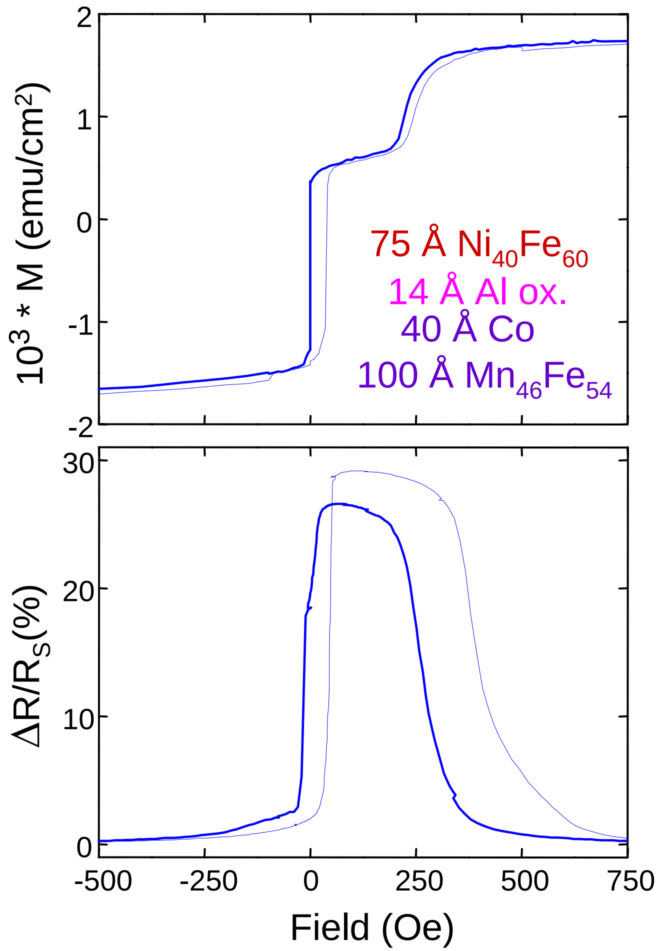

Hard Layer

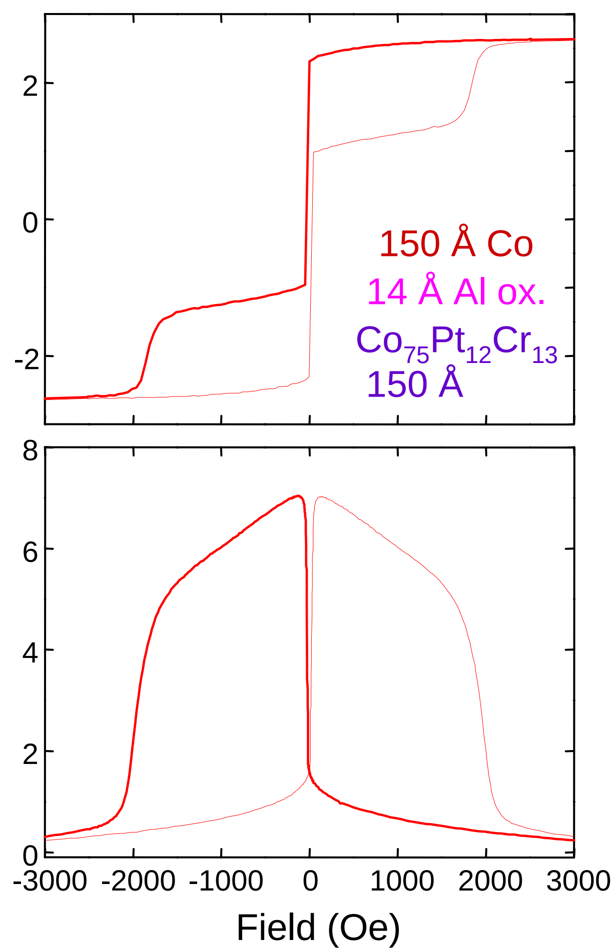

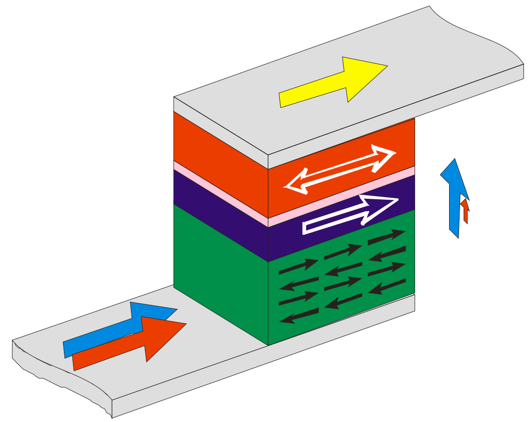

Exchange Biased

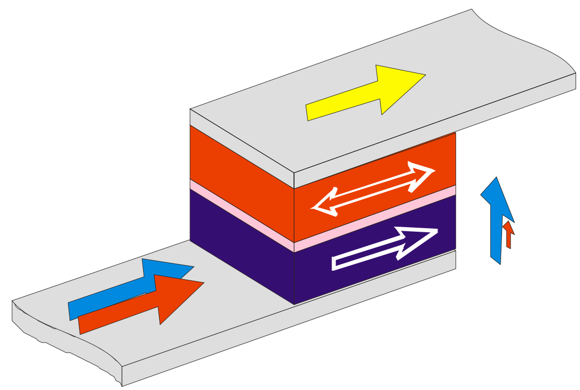

Hard/Soft

Stuart Parkin
July 7, 2003

Magnetization Creep in Hard/Soft MTJ

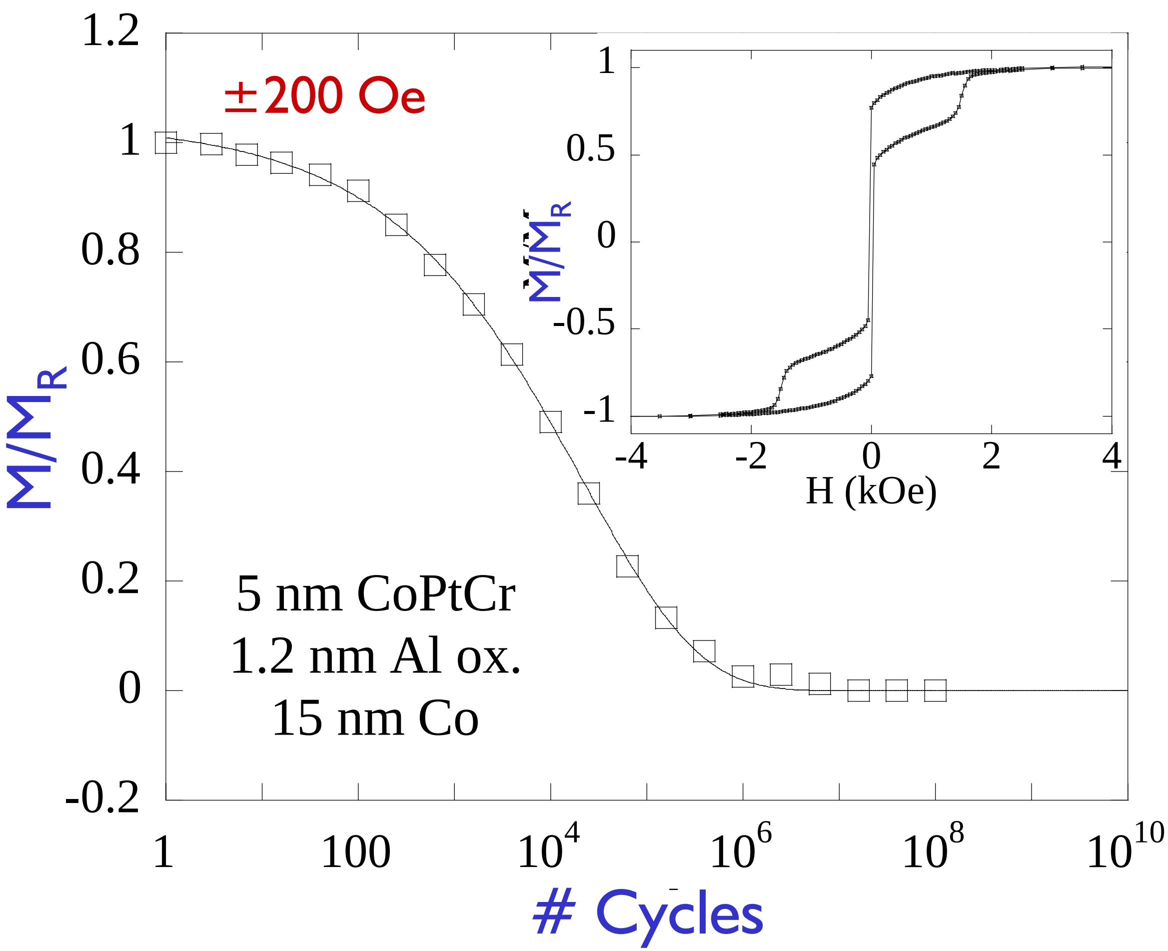

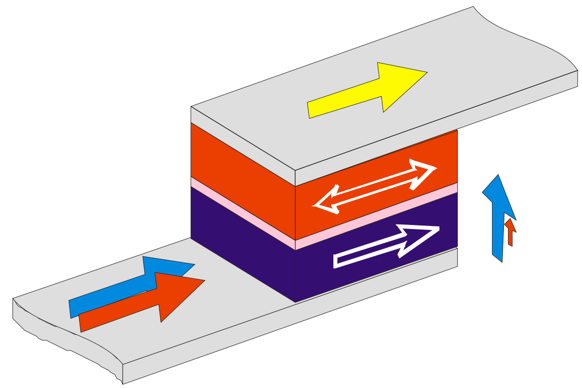

- Moment of hard layer decreases as moment of soft layer reversed
  - Eventually soft layer completely demagnetizes hard layer
- Remanent moment decay follows a stretched exponential curve
- Decay is independent of cycling frequency up to 10 kHz
- Exchange biased MTJs stable to field cycling

Stuart Parkin
July 7, 2003

Magnetization Creep in Hard/Soft MTJ

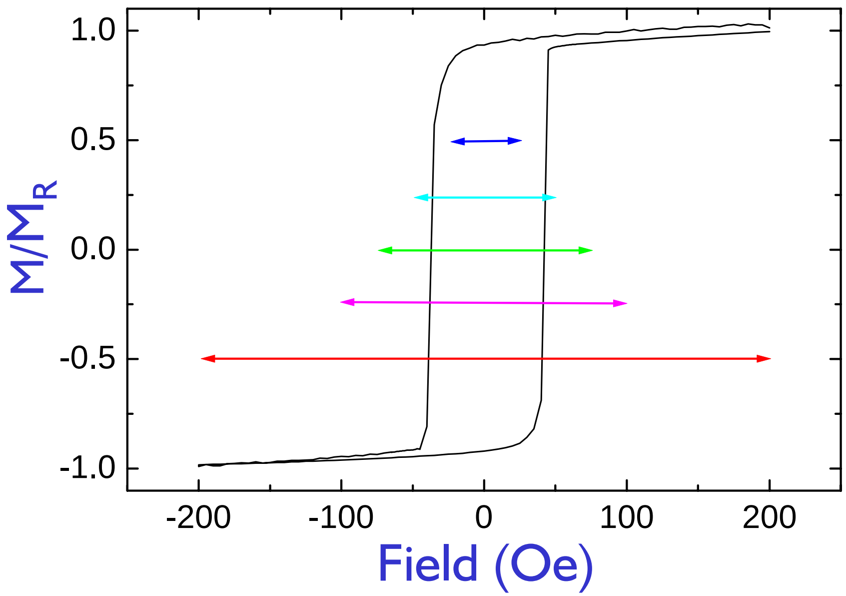

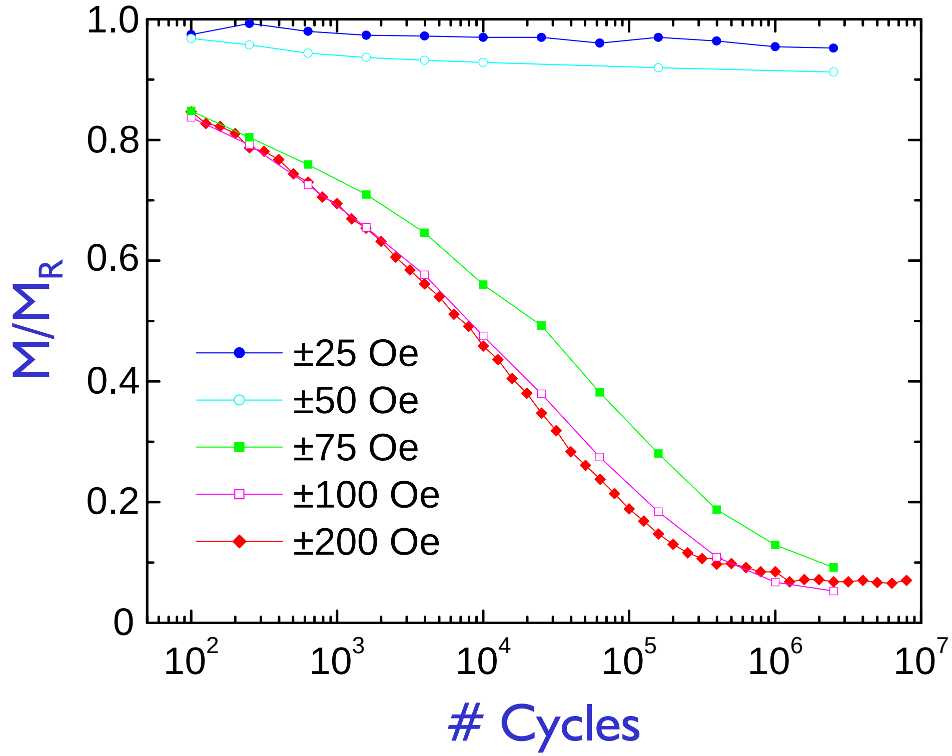

150 Å Co
12 Å Al ox.
20Å Co
100 Å $Co_{75}Pt_{12}Cr_{13}$

T=300 K: MTJ Set in 5 kOe: Cycled in ±25 to ±200 Oe

- Moment decay of hard layer caused by reversal of moment of free layer
  - No decay for fields smaller than coercive field of soft layer
  - Decay insensitive to field for field > H_c

Stuart Parkin
July 7, 2003

Dependence of Creep on Tunnel Barrier Thickness

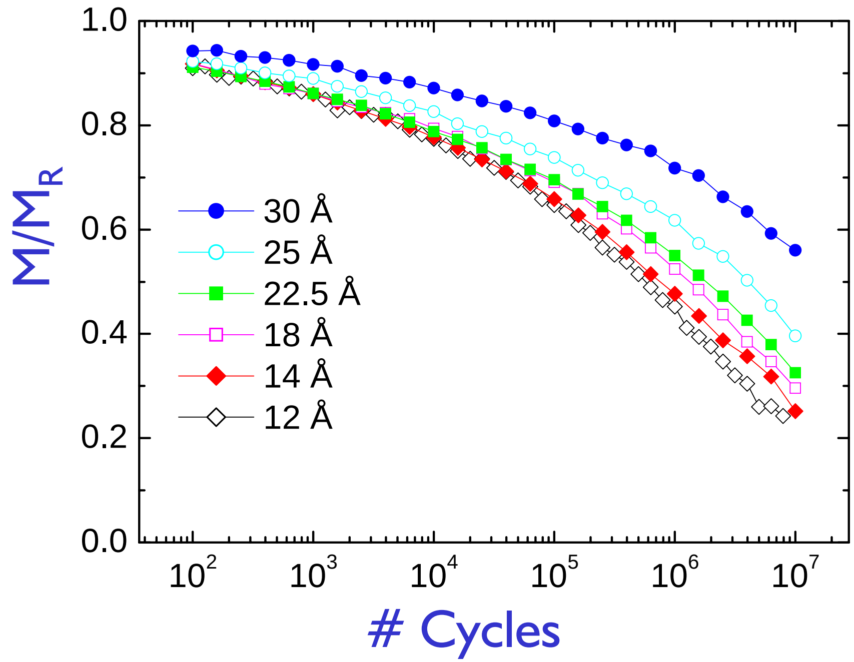

150 Å Co
x Å Al ox.
100 Å $Co_{75}Pt_{12}Cr_{13}$

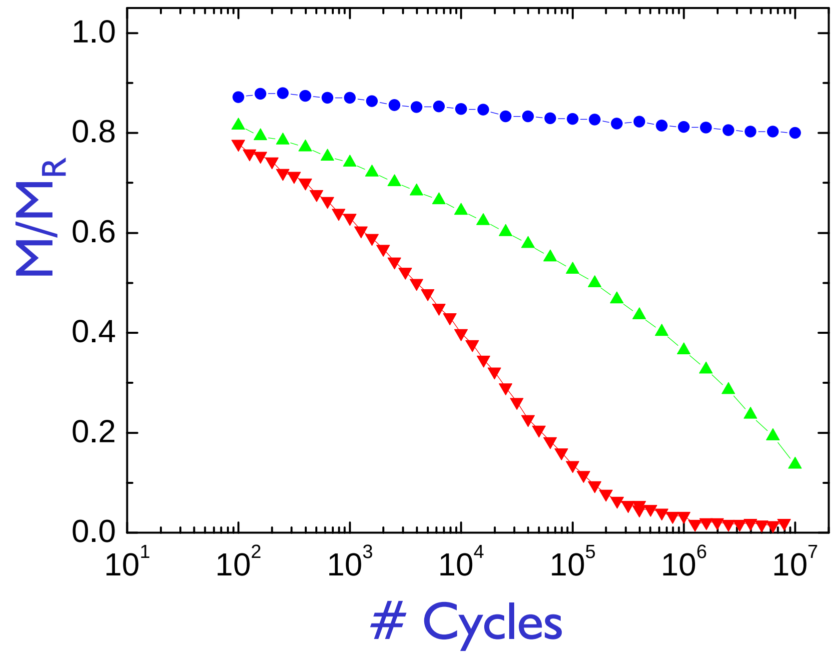

150Å $Ni_{40}Fe_{60}$
100 Å $Co_{75}Pt_{12}Cr_{13}$

150Å Co
100 Å & 200 Å $Co_{75}Pt_{12}Cr_{13}$

- Creep slower with increasing tunnel barrier thickness
- Creep faster for thinner hard layer
- Creep depends on magnetic properties of soft layer

T=300 K
MTJ Set in 5 kOe
Cycled in ±200 Oe

Stuart Parkin
July 7, 2003

Domain Wall Stray Field Magnitude

DW: top view

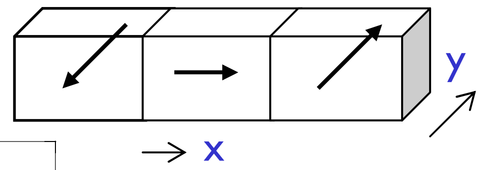

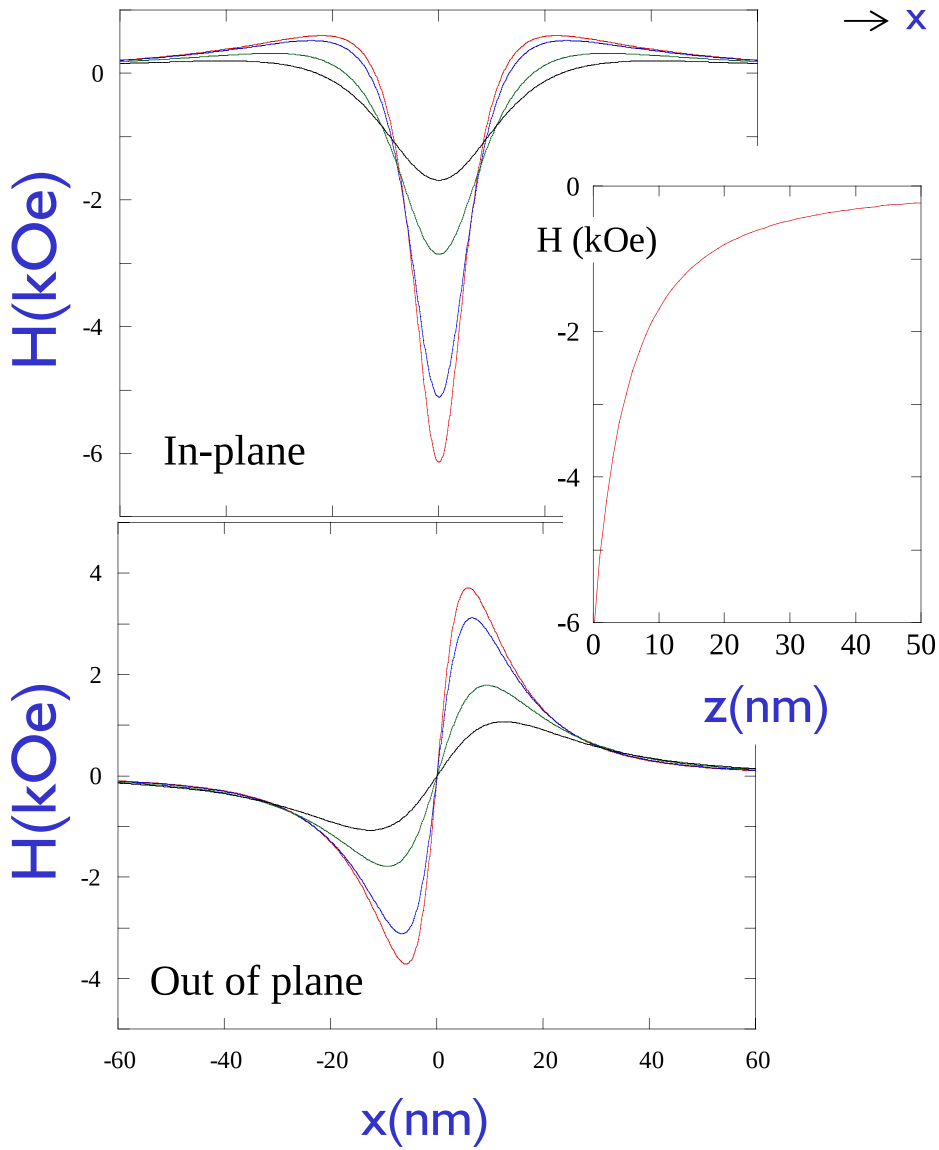

Thomas, Samant and Parkin, PRL (2000)

Stuart Parkin
July 7, 2003

Maximum Domain Wall Stray Field vs wall-width parameter, q

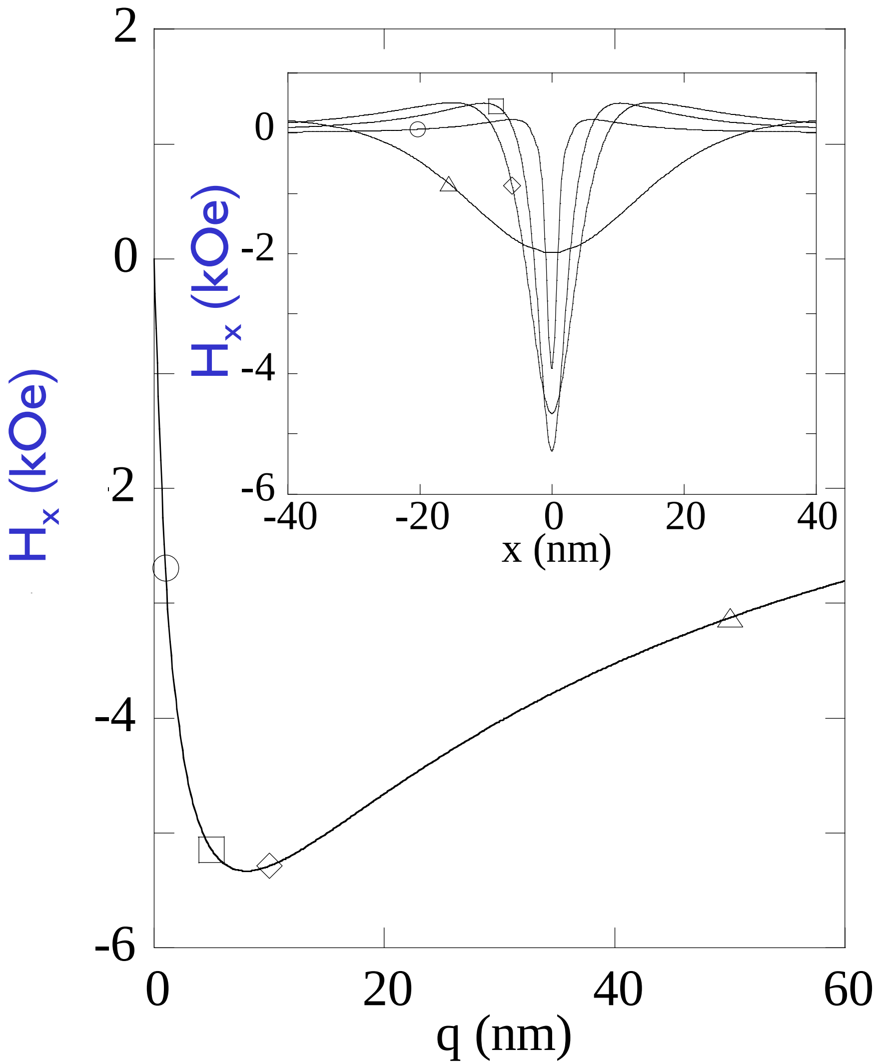

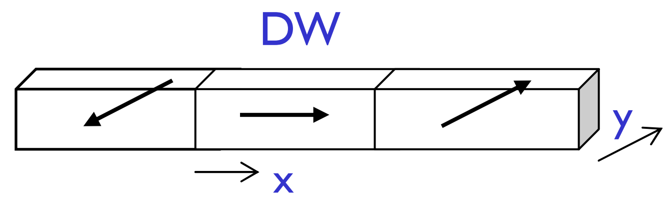

- DW stray field calculated from gradient of magnetic potential, Ψ(**r**)
  - For thin Co films DW likely to be of Néel type (M rotates in plane of film) and Ψ(r) depends on div M – no surface charge
  - Consider linear DW infinitely long along y (Dietze and Thomas)
    - M varies only along x; Ψ(**r**) related to M_x
    - $M_x(x)/M_S \sim q^2/(x^2+q^2)$ where q is a wall-width parameter

Thomas, Samant and Parkin, PRL (2000)

Domain Wall Fringing Fields

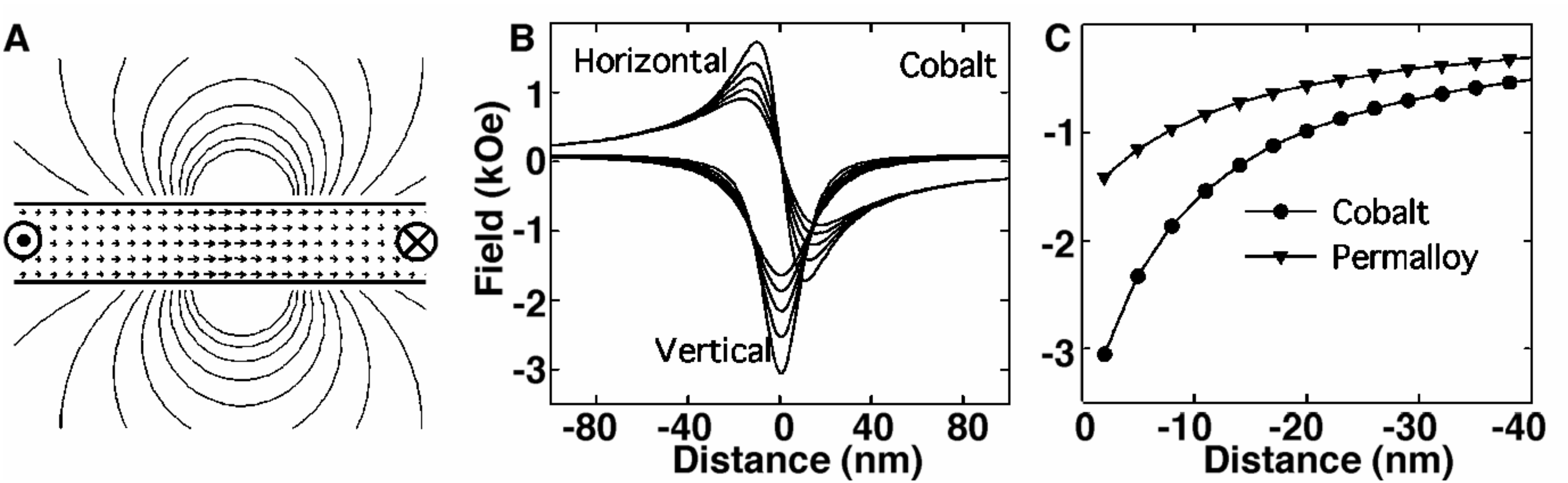

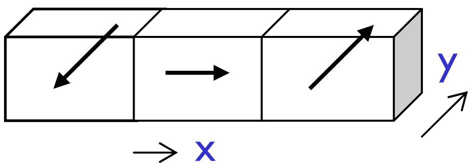

Mike Scheinfein

McCartney et al, Science (2000)

- very large stray fields from Neel wall in y and z directions

Origin of Creep in Hard/Soft MTJ

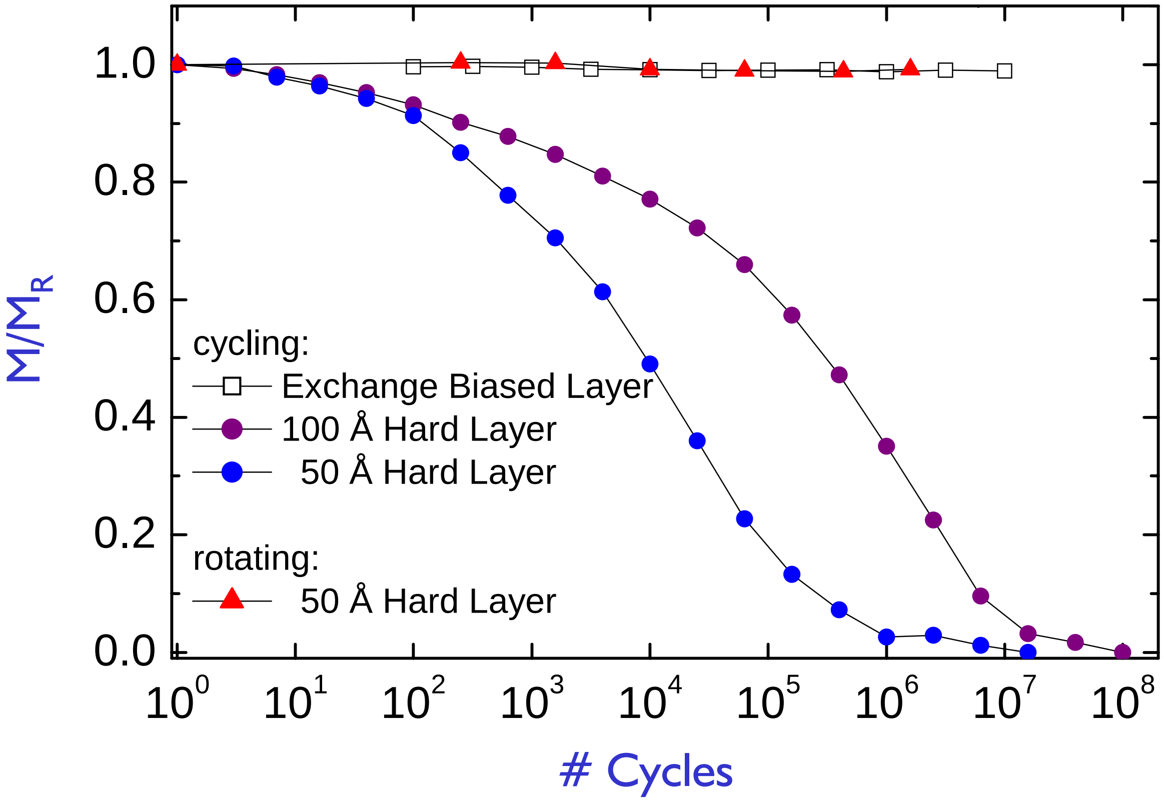

150 Å Co
12 Å Al ox.
20Å Co
100 Å $Co_{75}Pt_{12}Cr_{13}$

T=300 K
MTJ Set in 5 kOe
Cycled in ±200 Oe

- No creep of hard layer observed when moment of free layer rotated!
- Hard layer moment in CoPtCr/Al-O/Co MTJ sandwich:
  - decays to zero after reversing moment ~1,000,000 times
  - no creep after rotating moment ~1,000,000 times
- Mechanism via motion of domain walls in free layer
  - ☺ larger charge on domain walls in Co compared to $Ni_{40}Fe_{60}$

Magnetic Engineering at the Atomic Scale

MTJ exchange biased spin valve → **+ interface engineering** → **+ Artificial Antiferromagnet**

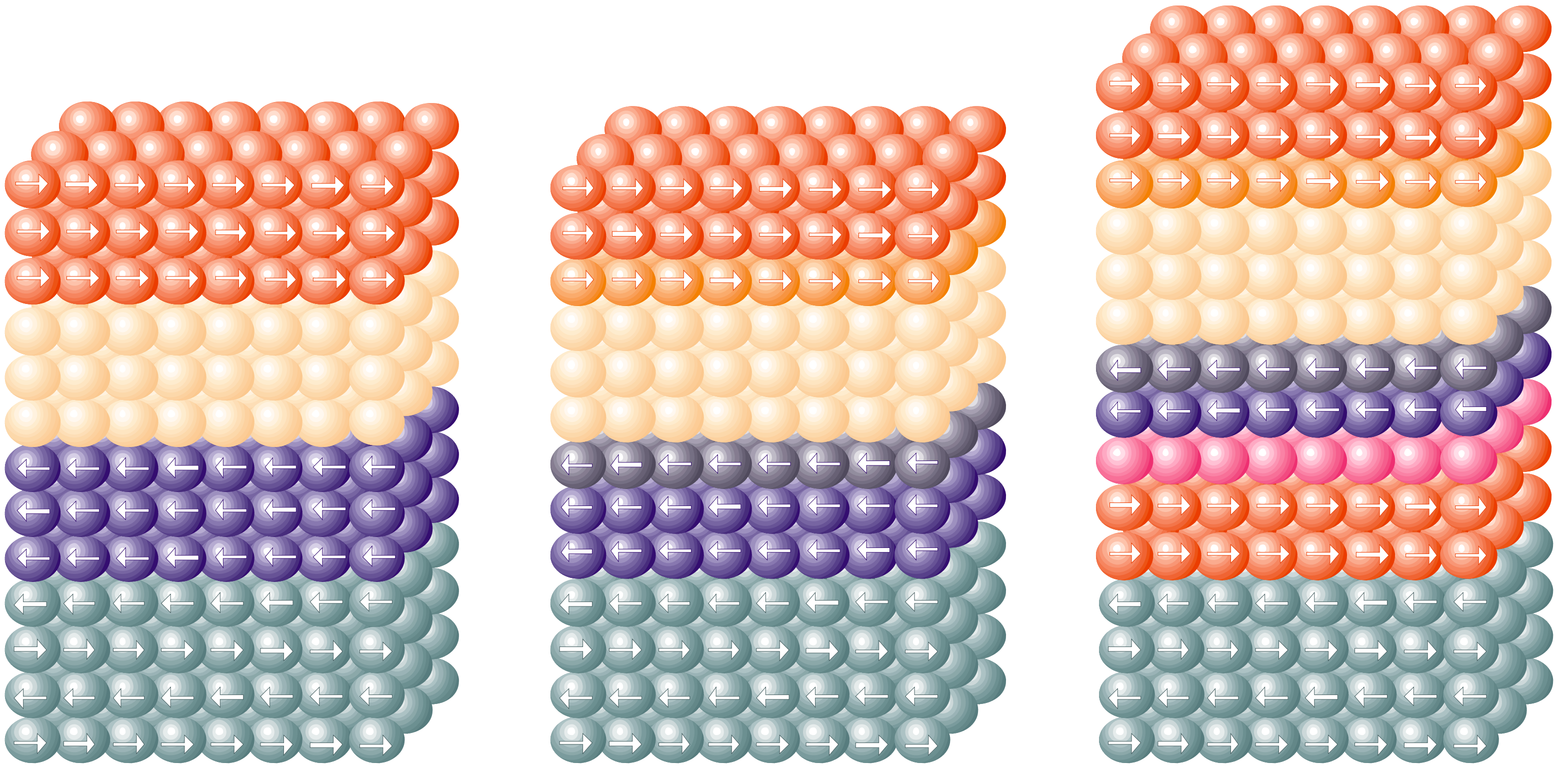

Stuart Parkin
July 7, 2003

Optical Characterization of Switching Uniformity

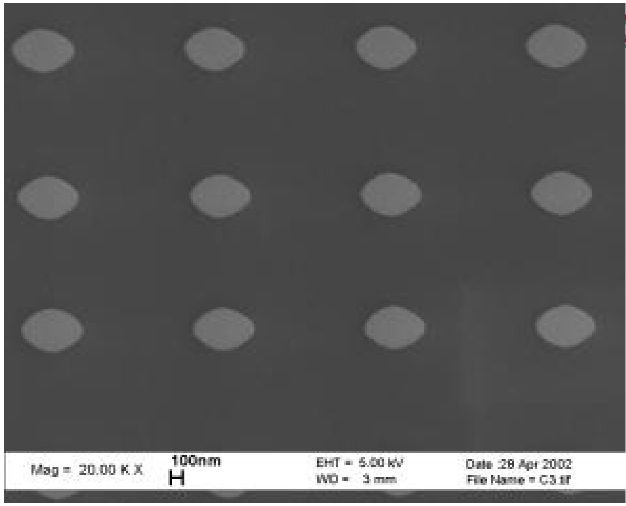

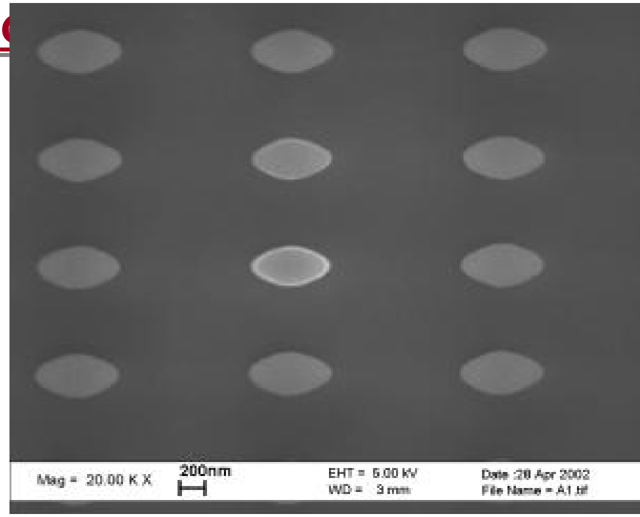

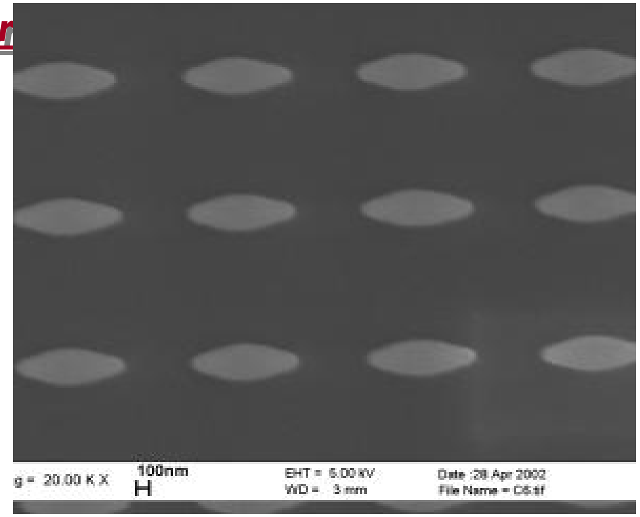

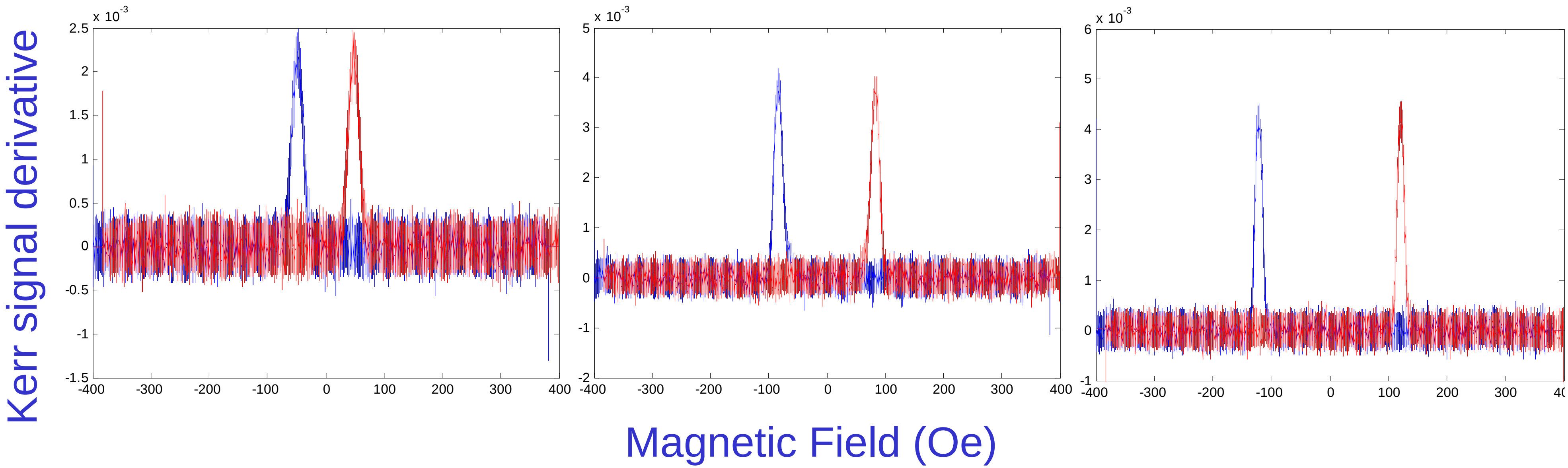

D.W. Abraham, P.L. Trouilloud et al.

Stuart Parkin
July 7, 2003

MTJ Magnetic Random Access Memory: Reading

- ☺ High resistance
- ☺ High magnetoresistance (MR)
- ☺ Controllable resistance
- ☺ Weak temperature dependence
- ☺ Scalable to small sizes with high MR
- ☹ MR falls off with increasing voltage

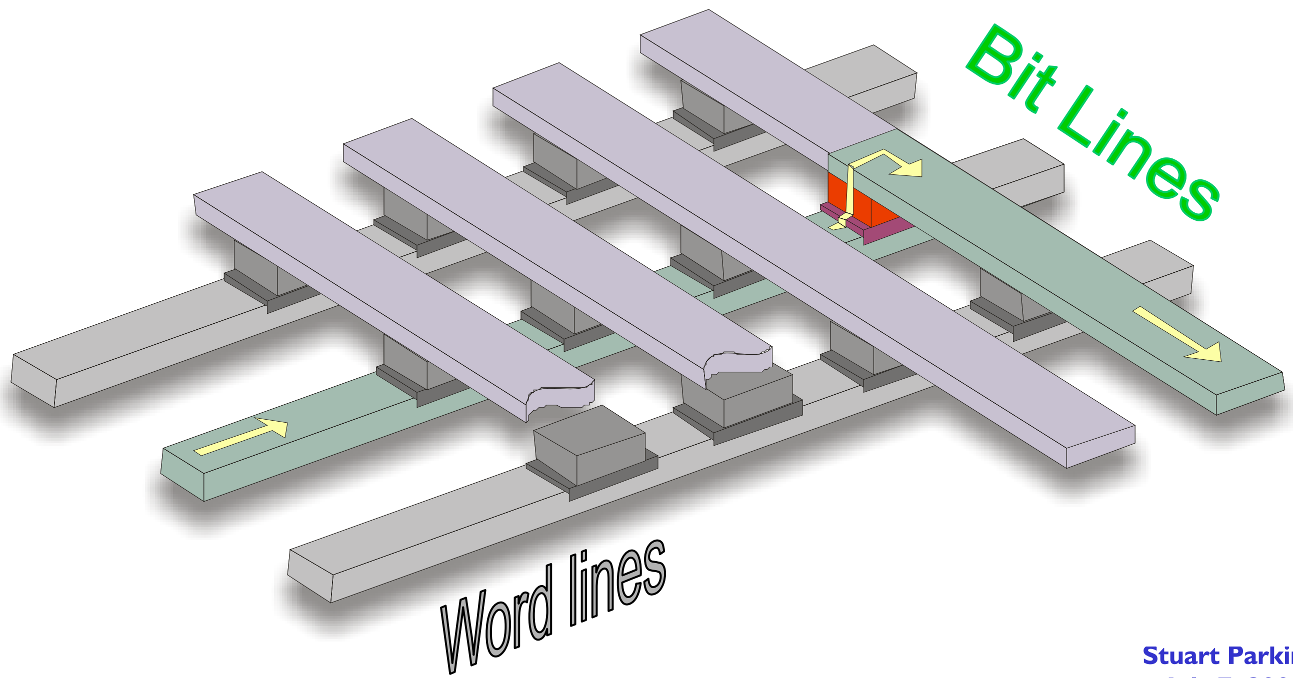

Stuart Parkin
July 7, 2003

Serial vs Crosspoint Architecture

Previous MRAMs
AMR, GMR: serial architecture

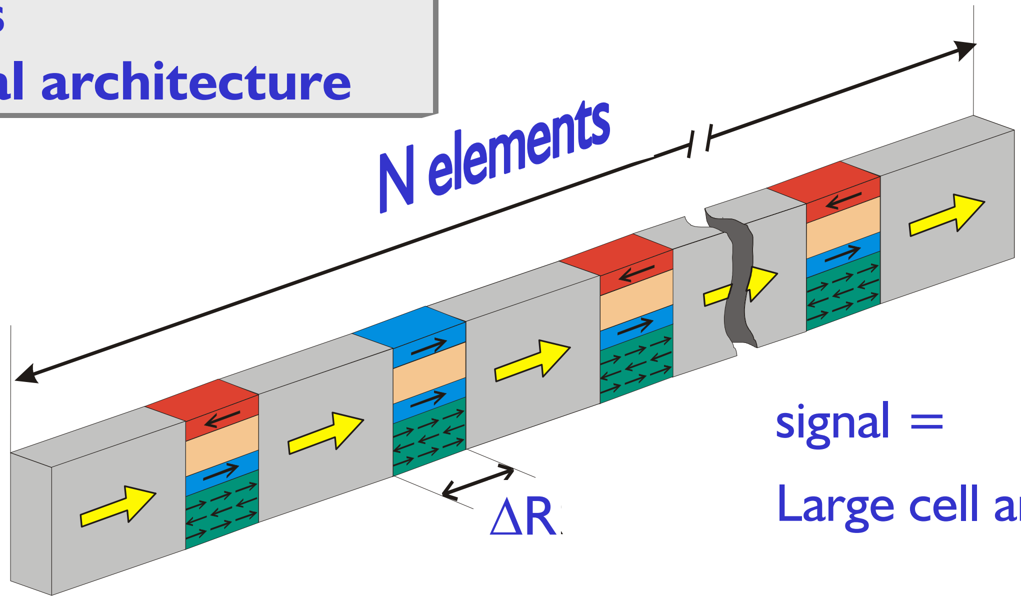

signal $= \dfrac{\Delta R}{N}$

Large cell area

MTJ: crosspoint architecture

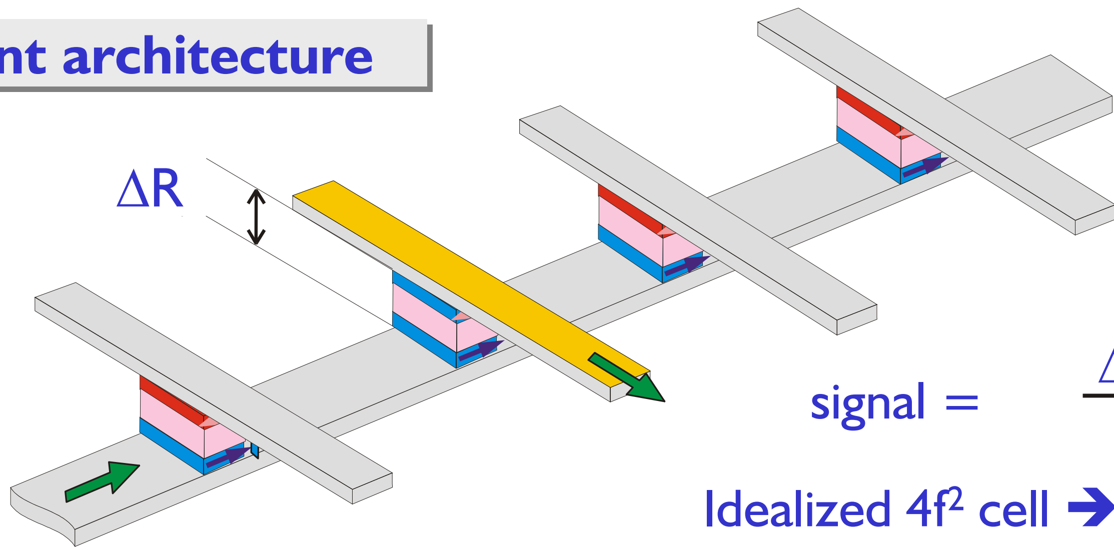

signal $= \dfrac{\Delta R}{1}$

Idealized $4f^2$ cell ➔ High density

MTJ MRAM: 1T-1R cell for Faster Reading

Reading

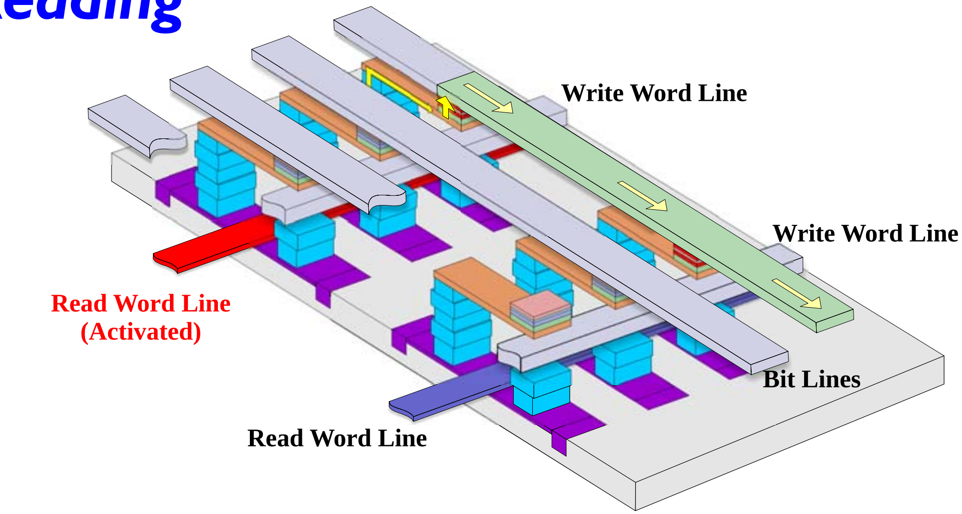

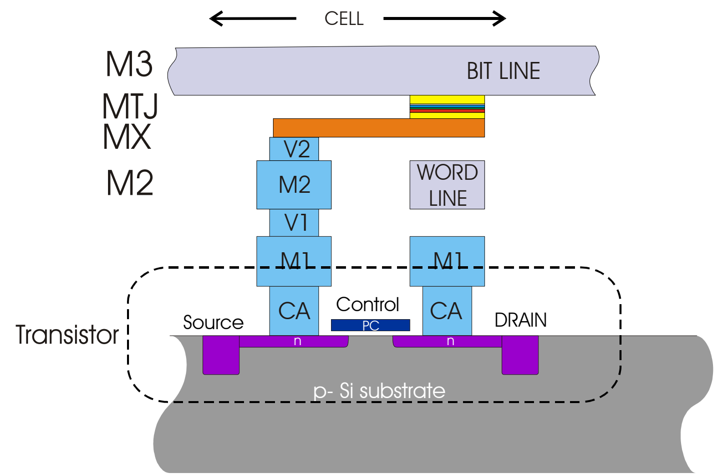

Writing

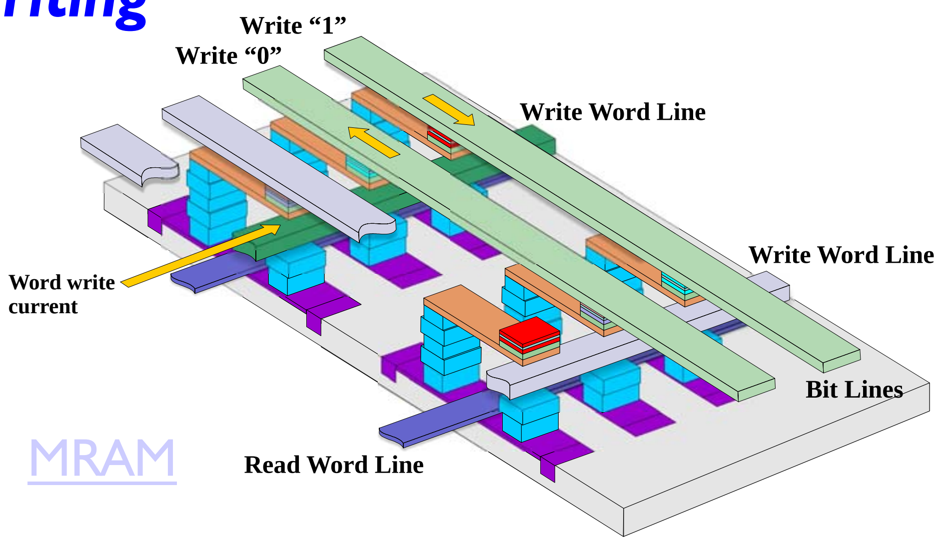

MRAM

Stuart Parkin
July 7, 2003

1 Transistor / 1 Resistor MRAM Cell

Reading

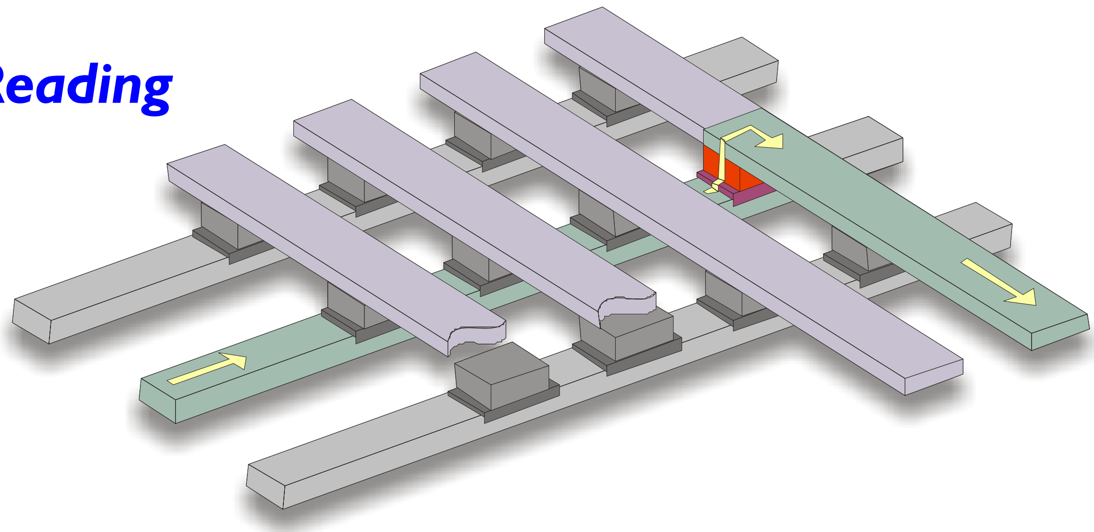

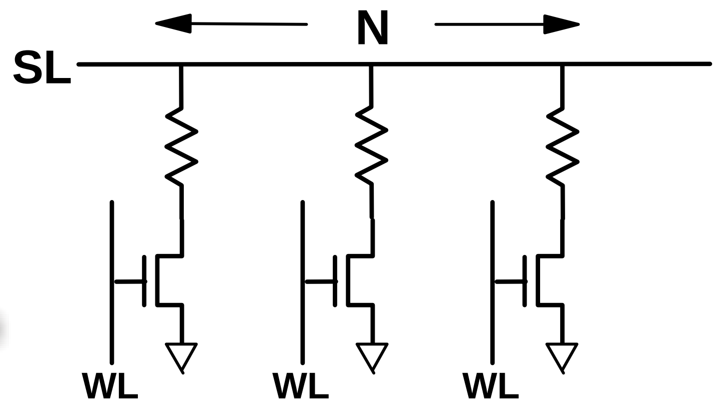

Signal ∝ MR/1 ➔ High performance

Sense power~10-100 fJ: 100,000 x smaller than GMR cell!

[higher MR, higher R and N~1]

~300 mV array voltage ➔ Low power

1T/1R increases size of cell

MRAM Cell Concepts

Cross point cell (1TJ)

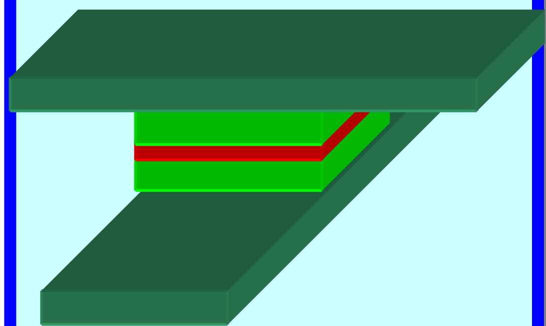

- Small cell area ($>4F^2/N$)
- Slower random access time [1]
- Flash like

[1] Dependent on array size

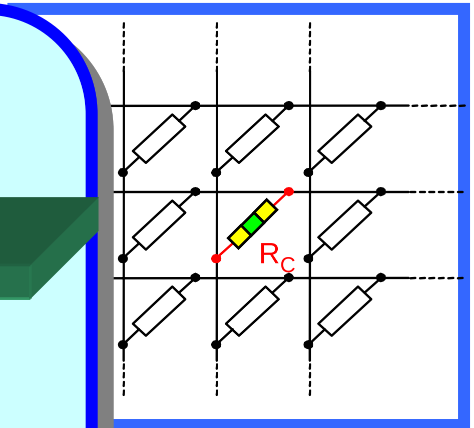

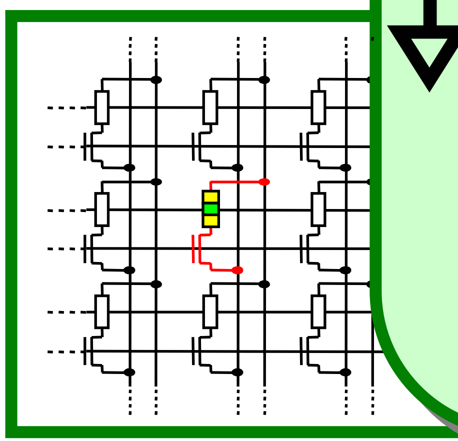

FET cell (1TJ-1T)

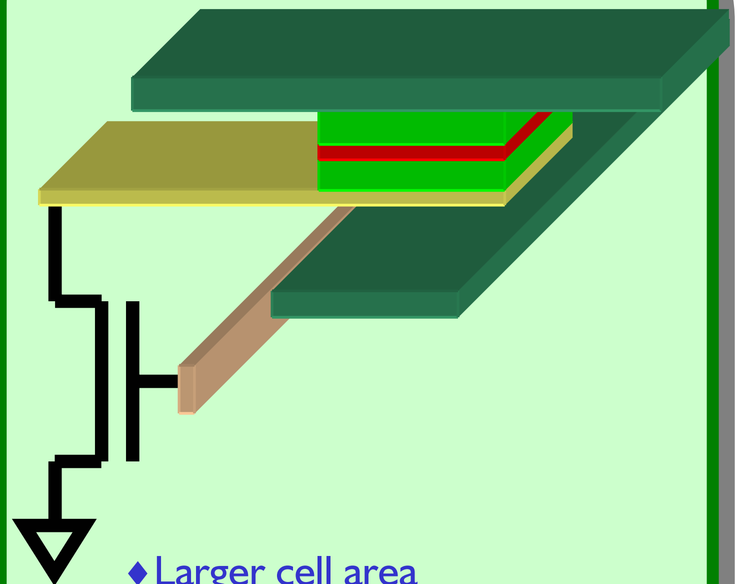

- Larger cell area ($>8\ F^2$)
- Faster random access time
- SRAM like ($\leq$10ns)

MTJ MRAM Demonstration

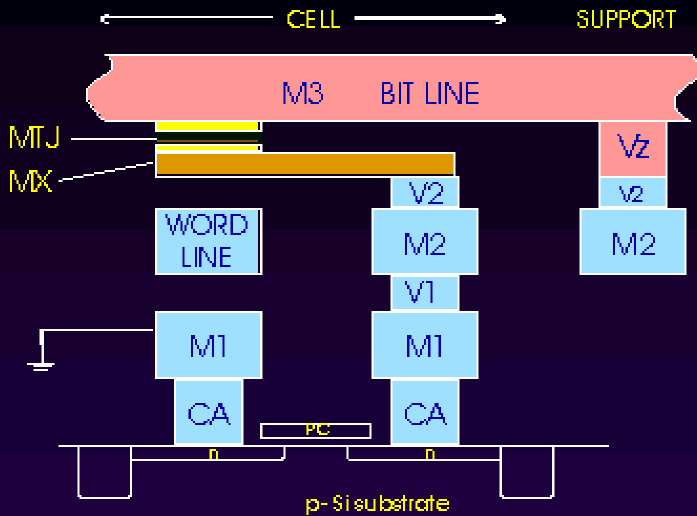

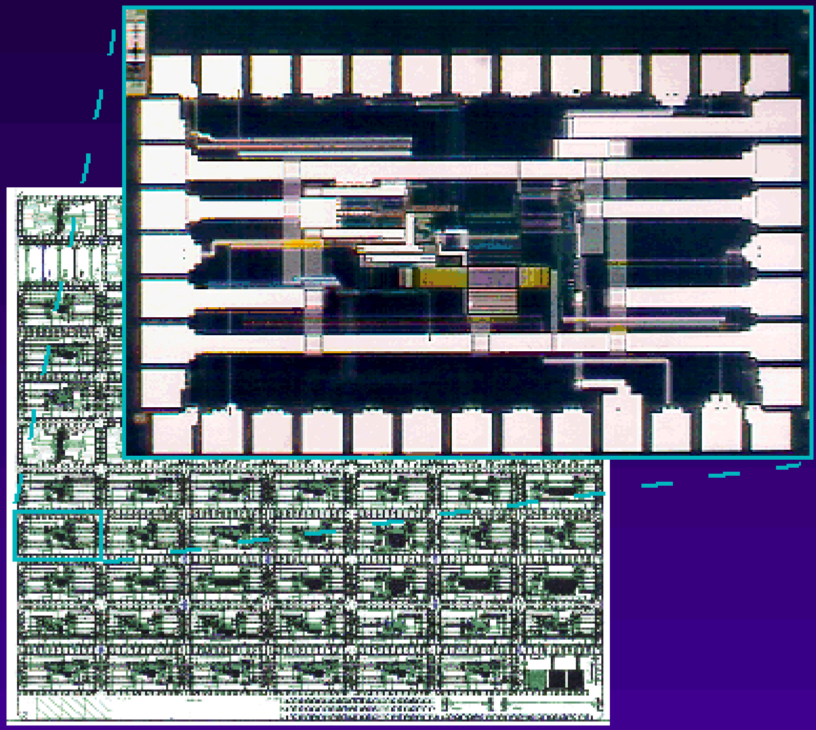

MTJ MRAM

As fast as SRAM, As dense as DRAM and
Non-volatile - no power needed to maintain memory

MRAM1 Characteristics

- 77 chiplets, 1 mm x 1.6 mm, 1K bit to 4K bit arrays
- Access time achieved: 2.25 ns
- Write time demonstrated: 2.3 ns
- Cycle time exercised: 10 ns (tester limited)

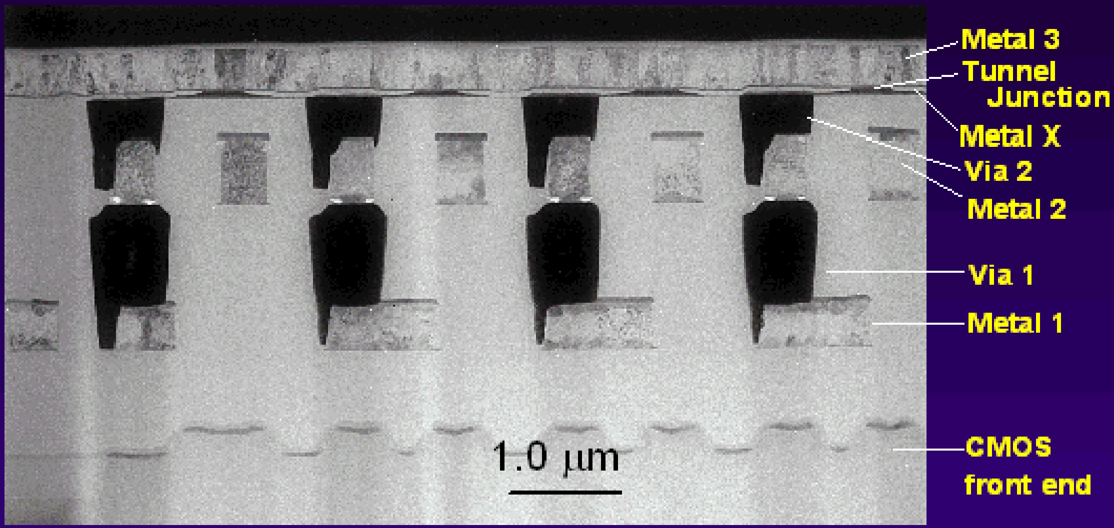

MRAM1 Processing

- CMOS 6SF fabricated in BTV on 200 mm Si, 3 special steps
- Wafers diced into 1" squares
- MTJ and MX materials (8 layers) deposited in Almaden
- MX, TJ, Vz, and M3 processed in Yorktown with e-beam lith

The MRAM Development Alliance

Formation: November 2000, IBM + Infineon
Mission:
Design and develop jointly a competitive and scalable MRAM technology.

→200mm MRAM technology development

→Cu BEOL technology

→Two architectures
- FET for high performance
- Cross point for high density

The MRAM Development Alliance

Project Locations

East Fishkill, NY
(main development site)

Yorktown Heights, NY

MRAM
Development Alliance

Almaden, CA

Burlington, VT

Erlangen

Stuart Parkin
July 7, 2003

Process Integration in 0.18μm Technology

Process Flow
Final Cu Level (M3)
2nd Cu Level (Bitline M2)
ILD, Planarization
Local Interconnect (MA)
MTJ Encapsulation
MTJ RIE Patterning
MTJ Stack Deposition
Contact Via (VA)
M1/VA ILD Deposition
1st Cu Level (Write Line M1)
0.18um CMOS fabrication

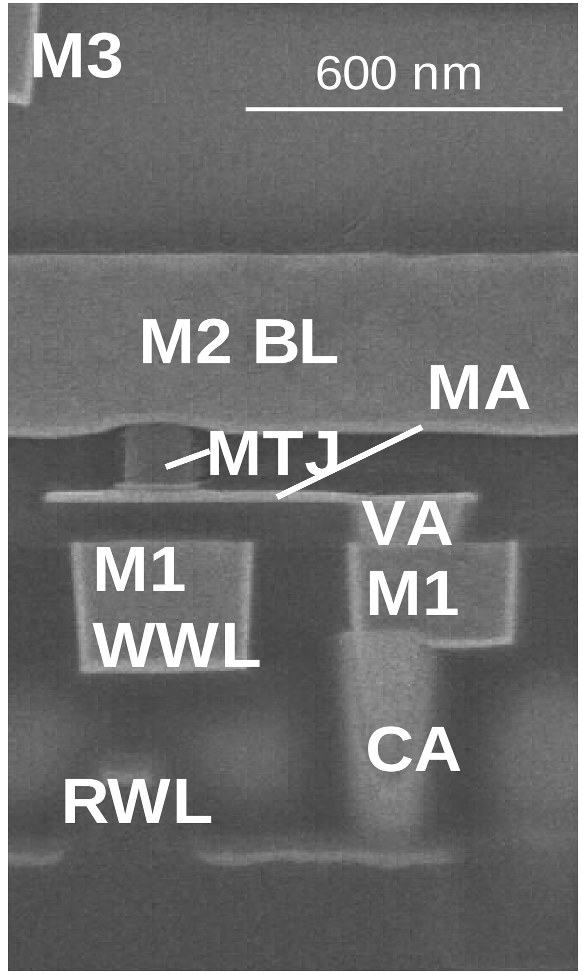

Key integration processes are:
- MTJ patterning by RIE
- Post etch treatment of the MTJ
- Encapsulation of the MTJ with a suitable low temperature ILD.

MTJ Control for Read Yield

Resistance distributions within a functional 2kbit array

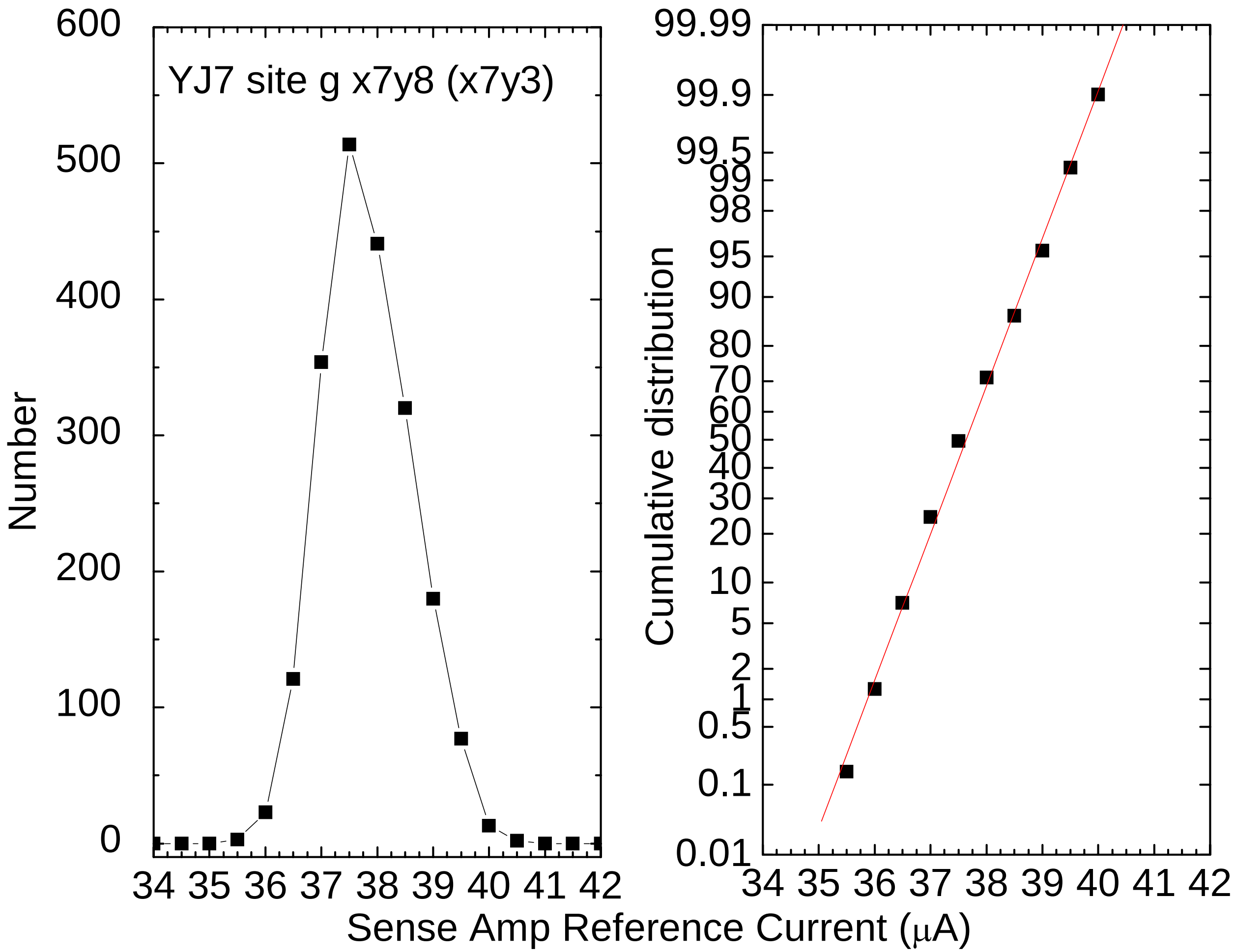

- 0.2×0.7 μm^2 MTJs
- Gaussian distribution
    - $\sigma_R \sim 2\%$
- No outliers

A. Sitaram, et al. VLSI Tech Symposium 2003

MTJ Control for Write Yield

Test Results Compared to Simulations

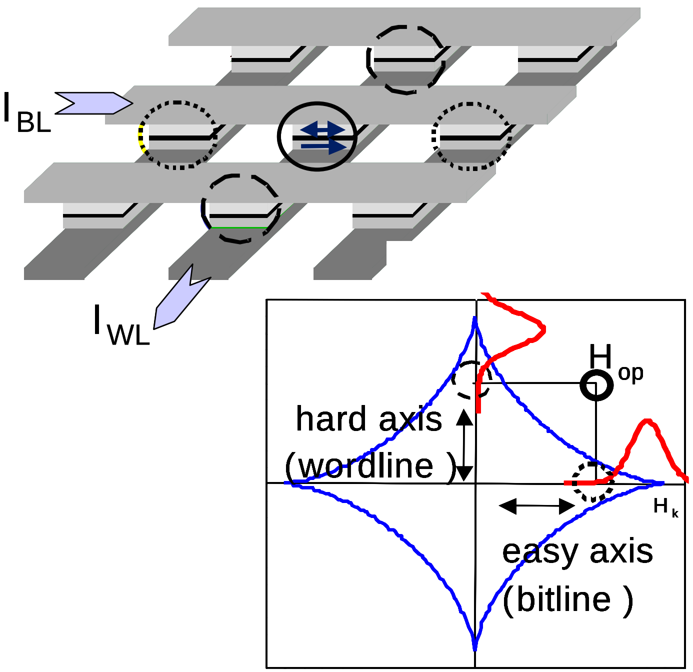

Array Quality Factor:

$AQF = H_{sw}/\sigma_{Hsw}$

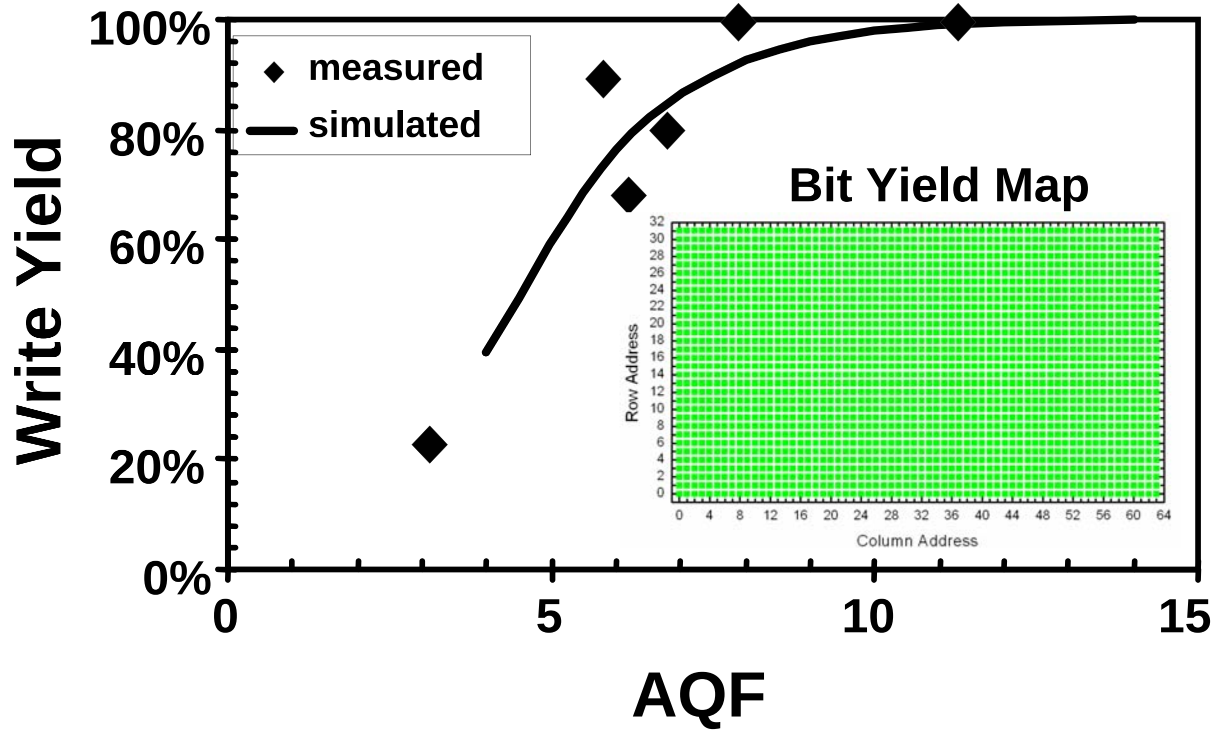

Write yield dependence on AQF:
Test results compared to simulations
(Inset shows checkerboard yield map for 2kbit array)

A. Sitaram, et al. VLSI Tech Symposium 2003

Endurance

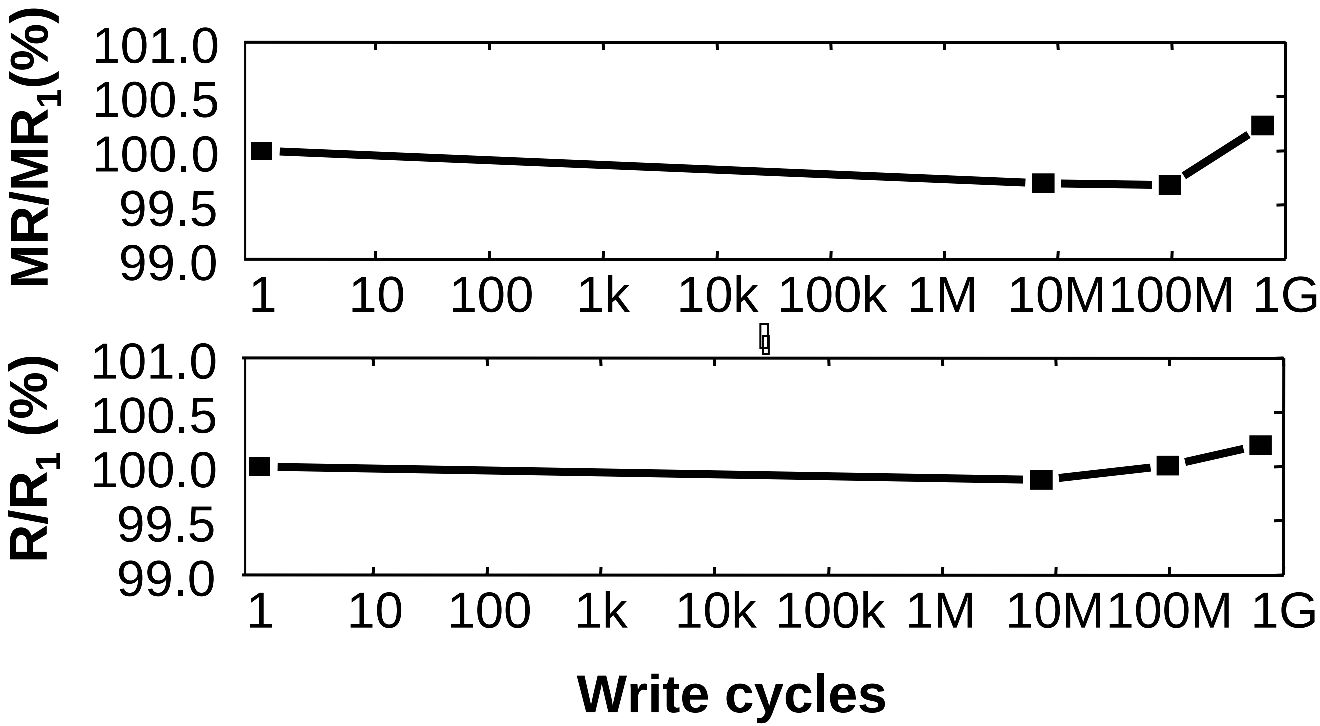

- Blanket write cycles on a 2kb array
- No significant degradation of median MR and MTJ resistance through 630 million cycles

128 kbit MTJ MRAM Core Array Fabricated in a 0.18 μm Cu Technology

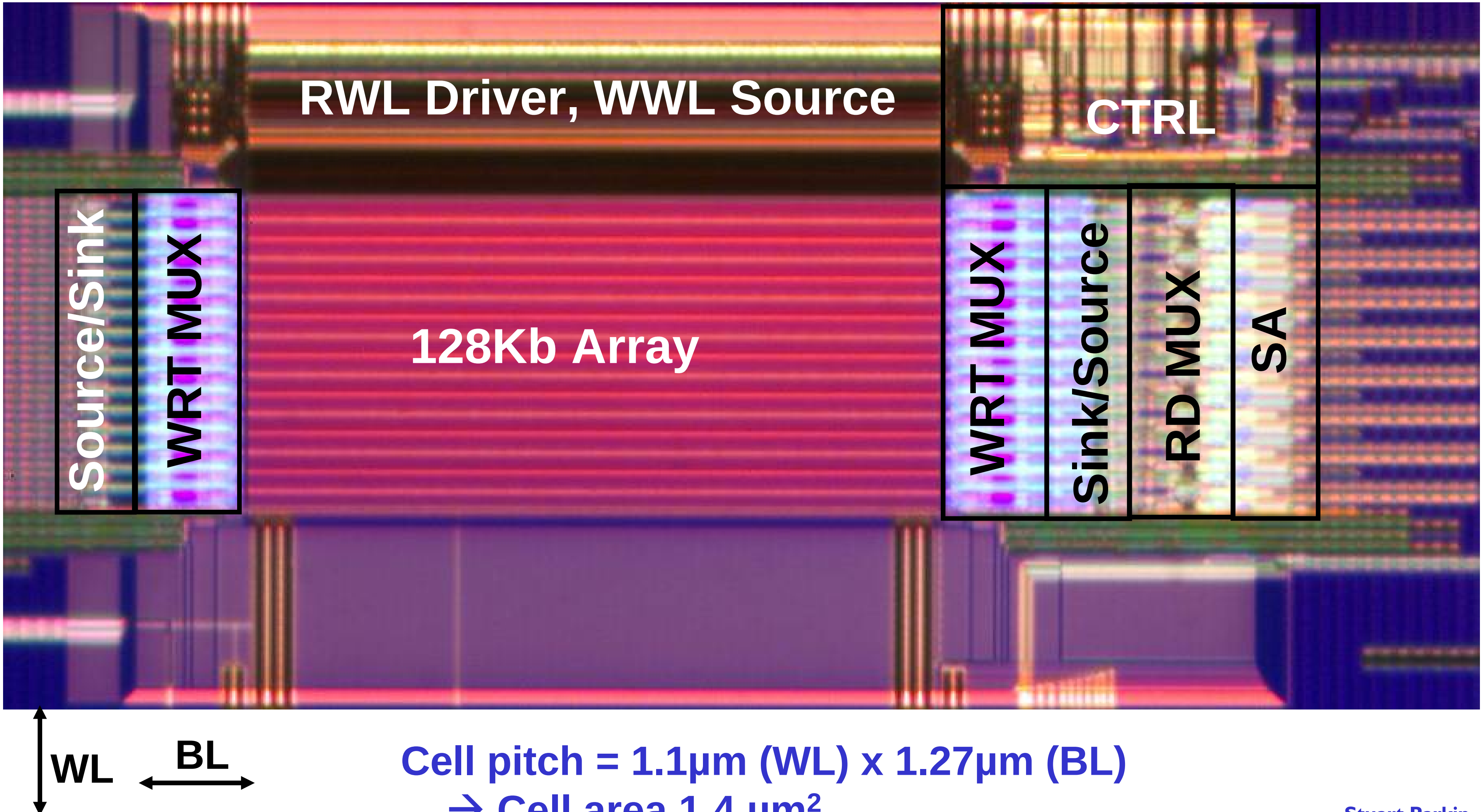

Cell pitch = 1.1μm (WL) x 1.27μm (BL)
→ Cell area 1.4 μm^2

A. Bette, et al. VLSI Circuit Symposium 2003

FET Cell Read Performance

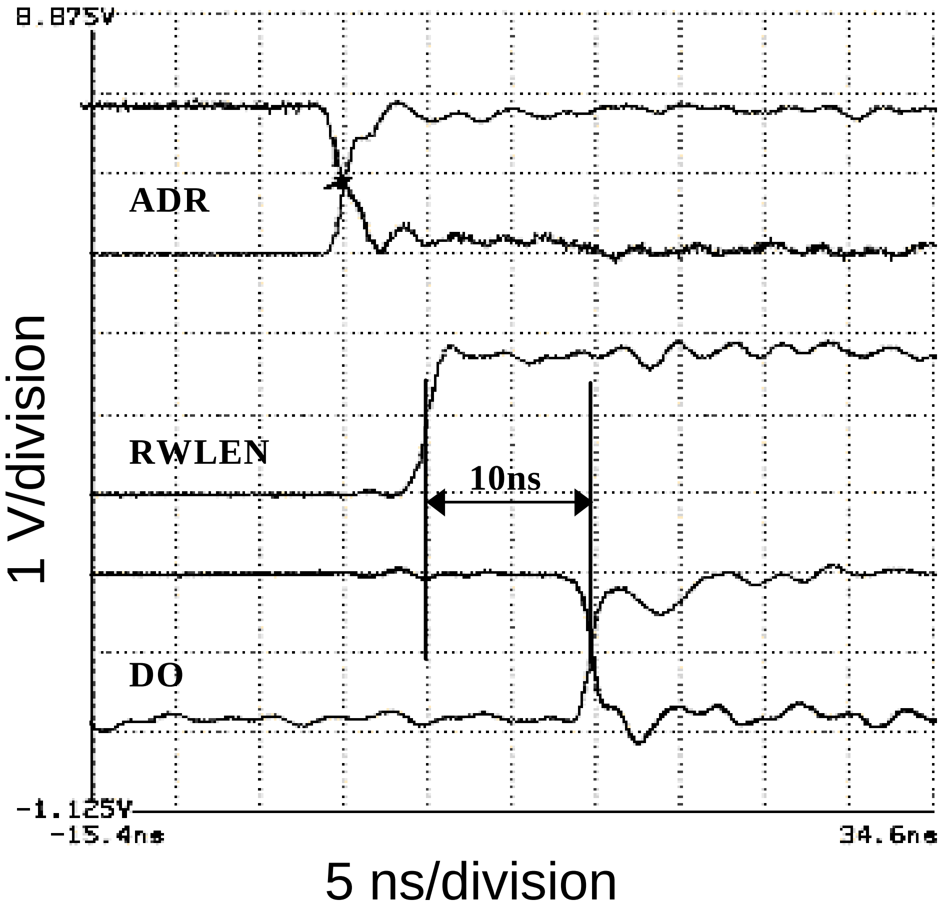

Array read access time measurement at 1.8V

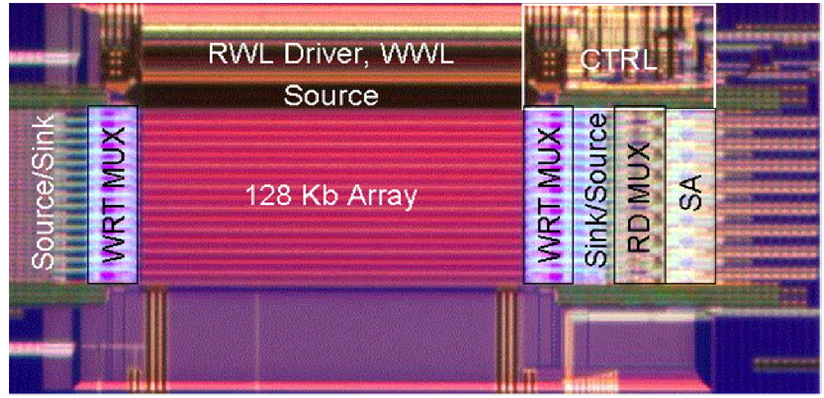

128 kbit FET MRAM test chip

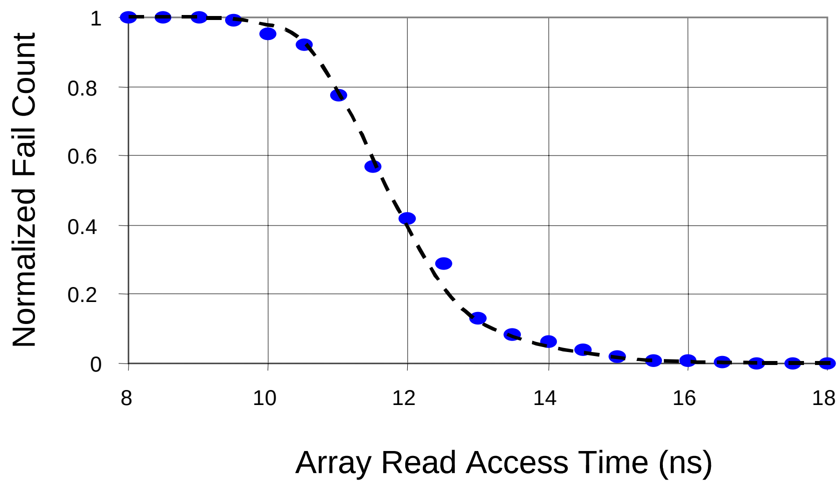

Measured distribution of access times

Performance Analysis of FET MRAM Read Operation

(Simulations, including margins)

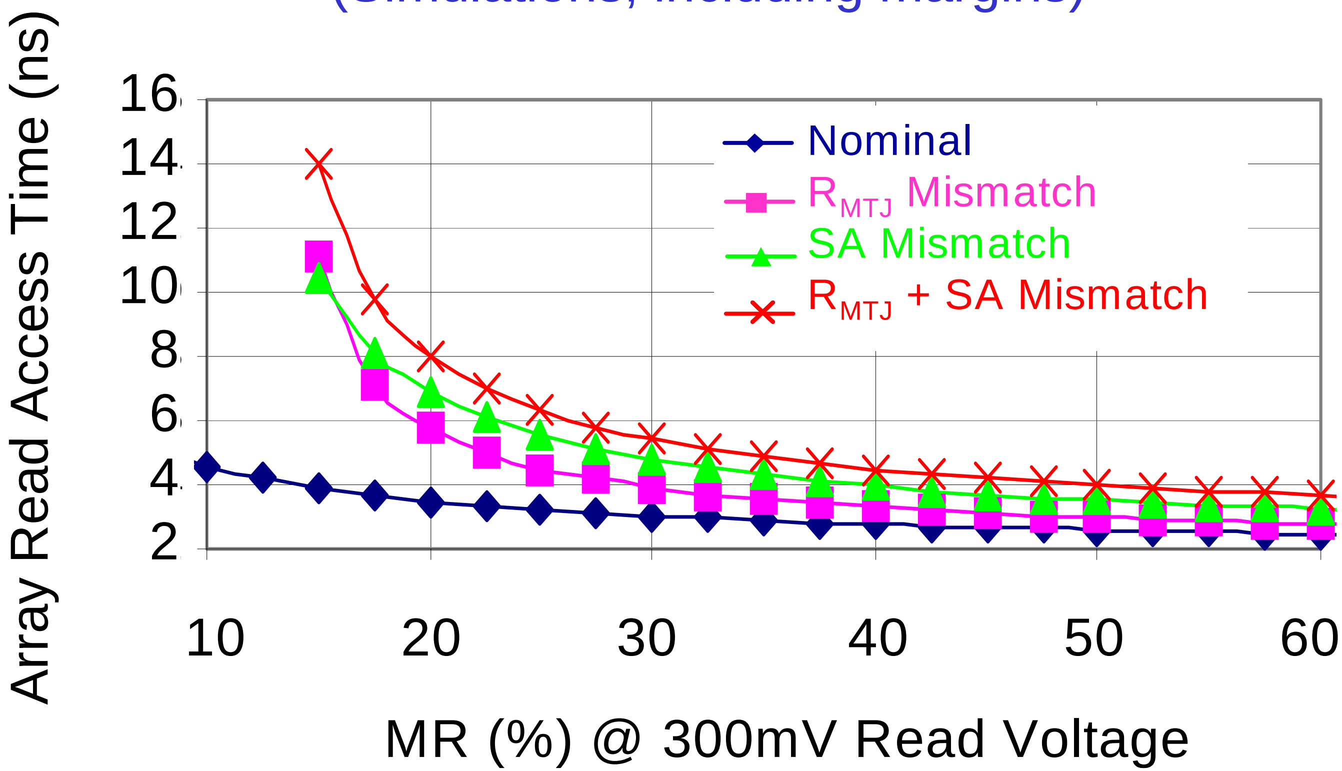

→ Through optimization of the MTJ resistance (R_L = 5 kΩ), optimization of the SA device matching and improvements in MR, a yieldable array read access time of 5ns is achievable with MR = 35% @ 300mV MTJ bias voltage.

A. Bette, et al. VLSI Circuit Symposium 2003

Time Required For Cell Writing

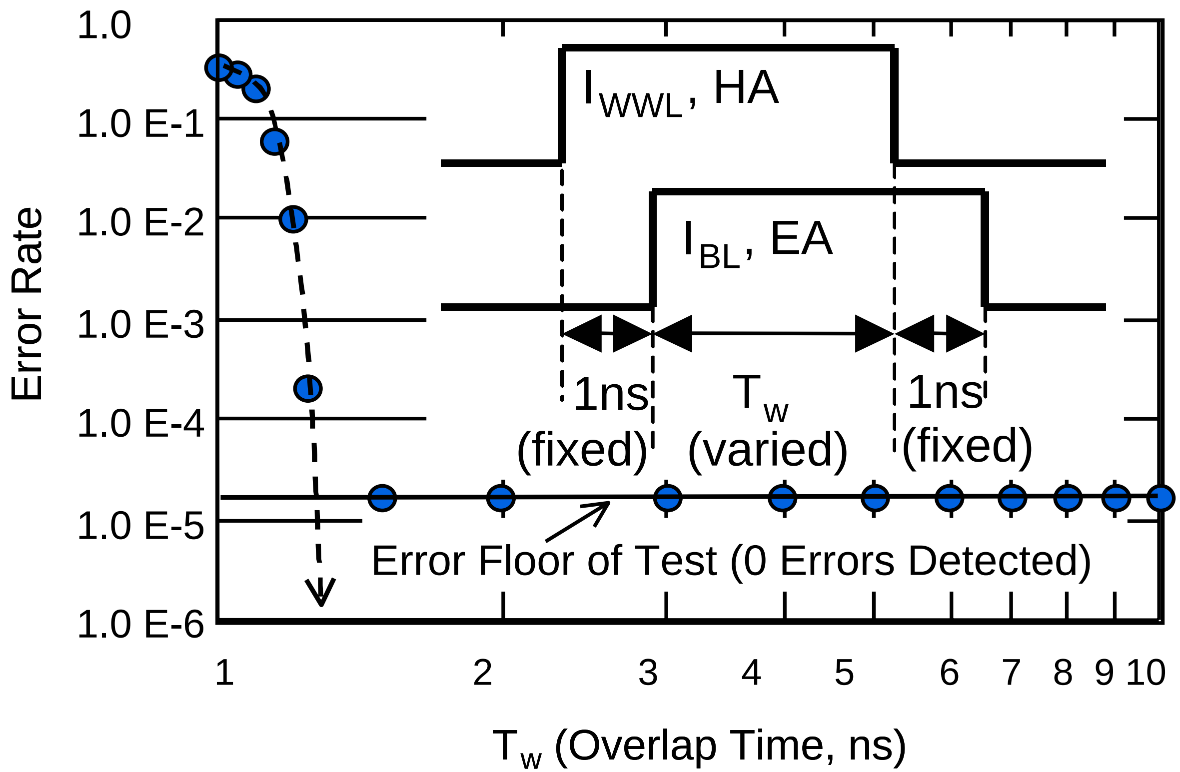

→ No errors observed beyond 1.5 ns T_w

Comparison of Memory Technologies

Existing Products	Technology Potential

	SRAM	DRAM	NAND Flash	NOR Flash	1T-1MTJ MRAM	XPC MRAM
Cell size in F^2	100	8	5	6	>8 [published: 20-40]	>4
Supply Voltage	2.5 V	2.5 V	1.8 V	3.3 V	1.8 V [published: 2.5-3.3V]	1.8 V
Retention Power	1μW-375 mW	10 mW	0	0	0	0
Retention Time	$\propto$ [with power]	64 ms	10 yrs	10 yrs	10 yrs	10 yrs
Random Read Access	2-100 ns	60 ns	10 μs	90 ns	10ns-50ns [published: 3ns–50ns]	50ns-1μs
Random Write Access	2-100 ns	60 ns	100 μs [erase 100 ms]	10 μs [erase 100 ms]	10-40 ns [published 3ns-50ns]	20-40 ns
Endurance	$>10^{15}$	$>10^{15}$	$>10^{15}$ read 10^5 write	$>10^{15}$ read 10^5 write	10^{15} [expected]	10^{15} [expected]

Magnetic Random Access Memory (MRAM)- The Perfect Memory!

DRAM is like a leaky bucket: Must be constantly refreshed to maintain contents

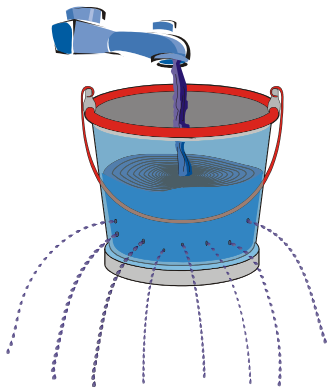

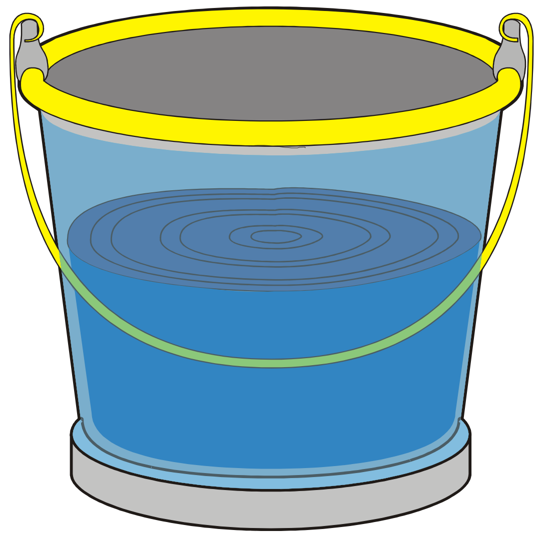

The SRAM bucket doesn't leak, but is a much bigger bucket

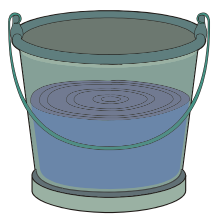

MRAM is a small bucket that does not need constant refilling